Origins of olivine in Earth's youngest kimberlite: Igwisi Hills volcanoes, Tanzania craton

Azhar M. Shaikh [a,*], Sebastian Tappe [a], Yannick Bussweiler [b], Christian Vollmer [b], Richard J. Brown [c]

[a] *Deep & Early Earth Processes (DEEP) Research Group, Department of Geology, University of Johannesburg, Auckland Park 2006, South Africa*

[b] *Institute of Mineralogy, University of Münster, Münster 48149, Germany*

[c] *Department of Earth Sciences, Durham University, Durham DH1 3LE, United Kingdom*

ABSTRACT

Nearly monomineralic several millimeter large rounded olivine nodules are common in kimberlites from localities worldwide. These polycrystalline nodules comprise either single or multiple anhedral olivine grains that are accompanied by smaller olivine neoblasts. It is generally thought that such 'dunitic nodules' originate from the base of the cratonic lithosphere and that their formation marks the onset of deep-rooted kimberlite magmatic plumbing systems, but thermobarometric constraints to support such a model have been lacking thus far.

In this study, we focus on the petrography and textural characteristics, as well as on pressure–temperature estimations, of exceptionally well-preserved dunitic nodules from the Quaternary Igwisi Hills kimberlite lavas on the Tanzania craton, with the ultimate goal to constrain their origins. We utilize EBSD-determined textural information in combination with olivine major and trace element data determined by EPMA and LA-ICP-MS methods to achieve this goal. We find that host olivine grains in these nodules are compositionally similar to olivine in garnet-facies cratonic mantle peridotites, and such a petrogenetic association is supported by rare garnet inclusions within olivine.

Projection of Al-in-olivine temperatures onto a regional cratonic geotherm suggests that the host olivine grains equilibrated at ~100-145 km depth, which points to origins from mid-lithospheric levels down to the lower cratonic mantle if a depth range of 160-180 km is considered for the present-day lithosphere–asthenosphere transition beneath the central Tanzania craton. These first pressure–temperature estimates for dunitic nodules in kimberlites suggest that their formation may also occur at significantly shallower depths than previously assumed for other occurrences worldwide.

Recrystallized olivine grains (i.e., neoblasts) show random crystallographic orientations and are enriched in minor and trace elements (e.g., Ca, Al, Zn, Sc, V) compared to the host olivine grains. These characteristics may link neoblast formation to melt-assisted in-situ recrystallization of cratonic mantle peridotite, a process that evidently persisted during kimberlite magma ascent through the lower half of thick continental lithosphere. Partial recrystallization of olivine-rich mantle xenoliths en route to surface increases the length of grain boundaries and also leads to the formation of abundant fractures within host olivine grains, which facilitates melt and fluid percolation that makes the xenoliths texturally weaker. Subsequent liberation of mineral grains from recrystallized peridotite xenoliths promotes the assimilation of compositionally ‘unstable’ orthopyroxene in rising carbonate-rich melts, which is considered to be an important process in the evolution of kimberlite magmas.

We show that dunitic nodules in kimberlites and related rocks may form as melt–rock equilibration zones along magmatic conduits within the lower half of the cratonic mantle column all the way up to mid-lithospheric depth levels. The dunitic nodules can be linked to certain types of olivine megacrysts, which are equally considered as melt/fluid-assisted recrystallization products of peridotitic mantle lithosphere along the ascent pathways of deep-sourced CO_2-H_2O-rich ultramafic melts.

Keywords: Kimberlite magma evolution, Olivine textures and compositions, Igwisi Hills volcanoes, Tanzania craton, East African Rift, Continental mantle lithosphere, EBSD

Introduction

Olivine is a ubiquitous constituent of kimberlites and some varieties may contain up to 60 vol.% of this mineral phase (Dawson 1971; Mitchell 1986; Kamenetsky et al. 2008; Brett et al. 2009; Arndt et al. 2010; Moss et al. 2010; Giuliani 2018). In coherent magmatic kimberlites, olivine occurs in the form of (i) anhedral to rounded discrete macrocrysts (0.5–10 mm) devoid of any recrystallization features, (ii) subhedral-to-euhedral phenocrysts (typically <1 mm), and (iii) rounded to subrounded dunitic nodules (generally 1–5 mm across) hosting abundant recrystallized olivine grains that are hereafter referred to as 'neoblasts'. Macrocrysts dominate among the olivine populations and their cores typically show evidence of deformation such as kink bands and undulose extinction. Together with evidence from mineral inclusions, the deformation features have been interpreted in light of lithospheric mantle origins of the olivine macrocryst cores (Kamenetsky et al. 2008; Brett et al. 2009; Bussweiler et al. 2015; Sobolev et al. 2015; Giuliani 2018), although Moore et al. (2020) considered this line of evidence as ambiguous and ascribed some of the olivine deformation features to the kimberlite magma ascent mechanism at crustal depths. In contrast, undeformed euhedral olivine phenocrysts often contain inclusions of other near-liquidus or even groundmass phases such as spinel, phlogopite and rutile (Kamenetsky et al. 2008; Bussweiler et al. 2015; Soltys et al. 2018). Although olivine phenocrysts can be abundant in some kimberlites (Mitchell et al. 2019; Soltys et al. 2020), the volumetrically most significant portion of magmatic olivine occurs as overgrowths on entrained olivine xenocrysts, such as the broad margins of most olivine macrocrysts.

Dunitic nodules in kimberlites are mm-sized polycrystalline olivine grains or aggregates that consist of multiple anhedral 'host' olivine grains, which are typically strained and enclose <0.5 mm large recrystallized olivine subgrains (i.e., neoblasts). According to Arndt et al. (2010) and Cordier et al. (2015), all subrounded to rounded mm-sized olivine grains in kimberlites and related rocks should be called ‘dunitic nodules’, a view that we do not share for several reasons, as will be discussed in this paper. Herein, we do not consider sizable discrete olivine crystals without any neoblasts as ‘nodules’, but rather consider those as ‘macrocrysts’. The undeformed subgrains in dunitic nodules are either rounded or polyhedral ‘neoblasts’. Elongated subhedral-to-euhedral neoblasts with asymmetrical faces are commonly referred to as ‘tablets’ (Boullier and Nicolas 1975; Guéguen 1977; Mercier 1979; Green and Guéguen 1983; Arndt et al. 2010; Tappe et al. 2021). In this study, all recrystallized olivine grains in dunitic nodules, regardless of whether they are anhedral, subhedral or euhedral, are collectively referred to as ‘neoblasts’ (Fig. 2c-d).

Two main compositional types of olivine xenocrysts are known from kimberlites and related rocks worldwide; i.e., Mg-rich and Fe-rich (Kamenetsky et al. 2008; Brett et al. 2009; Arndt et al., 2010; Pilbeam et al. 2013; Bussweiler et al. 2015; Howarth and Taylor 2016; Moore and Costin 2016; Giuliani 2018; Lim et al. 2018; Dongre and Tappe, 2019; Shaikh et al. 2019; Soltys et al. 2020). Arndt et al. (2010) argued against such a bimodal distribution of ‘kimberlitic’ olivine compositions and instead suggested the existence of a compositional continuum between the two main recognized endmembers. The Mg-rich olivine xenocrysts are generally considered to be sourced from cratonic mantle peridotites, whereas the Fe-rich olivine xenocrysts are linked to the products of melt-related mantle metasomatism such as olivine megacrysts and sheared peridotites (Brett et al. 2009; Bussweiler et al. 2015; Howarth and Taylor 2016; Moore and Costin 2016; Giuliani 2018).

The origin of dunitic nodules in kimberlites and related rocks is a matter of active debate. Arndt et al. (2010) proposed a model in which dunitic nodules form by the removal of pyroxenes and garnet from four-phase peridotite during interactions with proto-kimberlite melt at the base of cratonic mantle lithosphere. This process was termed ‘defertilization’ and argued to be an important precursor mechanism that aids kimberlite magma ascent through the overlying lithosphere (Arndt et al. 2010; Cordier et al. 2015). Other studies pointed out that dunitic nodules may be sourced from coarse-grained peridotites and olivine megacrysts (Giuliani and Foley 2016; Moore 2017). Rooney et al. (2020) suggested that dunitic nodules in aillikites from the Superior craton formed by fusion of metasomatic carbonate and phlogopite components within peridotite at the base of cratonic mantle lithosphere. It must be noted, however, that links between dunitic nodules and the lowermost cratonic mantle lithosphere have not been tested yet by the application of modern pressure–temperature estimates (hereafter P–T).

In this study of exceptionally fresh kimberlite lavas from the Igwisi Hills in Tanzania, we employed a combined approach to examine the possible origins of dunitic nodules, which includes petrographic–textural analysis by the electron backscatter diffraction method (EBSD), as well as major and trace element analyses of olivine by EPMA and LA-ICP-MS techniques. Our results reveal that dunitic nodules from the Igwisi Hills kimberlite volcanic system formed at significantly shallower, mid-lithospheric depths compared to previous models for similar materials that placed their origin exclusively at the base of cratonic mantle lithosphere (e.g., Arndt et al. 2010; Cordier et al. 2015; Rooney et al. 2020). Textural observations from the dunitic nodules and discrete olivine macrocrysts enable us to further constrain kimberlite magma evolution. This also includes possible links between dunitic nodules and olivine megacrysts, which may hold clues to the workings of kimberlite and similar deep-sourced volatile-rich magmatic systems such as aillikites.

The Quaternary Igwisi Hills kimberlite volcanic system

The modern Igwisi Hills kimberlite volcanoes (4°53′19.22″ S, 31°55′59.15″ E) are located at the western margin of the Tanzania craton (Fig. 1), where the magmas erupted through gneisses of the Archaean Dodoman system (Bell and Dodson 1981). The volcanoes comprise three exceptionally well-preserved sub-circular volcanic centres (NE, Central and SW volcanoes), which contain pyroclastic rocks and lava flows at the crater margins, plus sediments in the crater centres (Fig. 1). The lava flows contain variable proportions of olivine-dominated micro-xenoliths (Dawson 1994), referred to here as ‘dunitic nodules’ to conform with recent developments in kimberlite petrology (Arndt et al. 2010). The dunitic nodules are set in a calcite-rich groundmass that also contains abundant spinel-group minerals, perovskite and apatite (Willcox et al. 2015). With magma eruption ages between 12.4 ±4.8 ka and 11.2 ±7.8 ka, the Igwisi Hills volcanic system represents the youngest known kimberlite on Earth (Brown et al. 2012), and its ultimate origin has been linked to tectonic stresses imposed onto the Tanzania craton by the surrounding active East African Rift System (Tappe et al. 2018).

Whether or not the lava flows at the Igwisi Hills are true kimberlites has been debated. Mitchell (1970) used the absence of mantle-derived garnet and Cr-diopside xenocrysts as an argument against a kimberlitic affinity of the Igwisi Hills lavas. On the basis of mineralogy and bulk rock compositions, Reid et al. (1975) and Dawson (1994) identified the Igwisi Hills lava flows as calcite kimberlite, a variety that has higher CO_2/H_2O compositions than more typical H_2O-rich hypabyssal kimberlites, which are more common on a global scale (Kjarsgaard et al. 2009). More recent mineralogical and geochemical studies reiterate the kimberlitic nature of the Igwisi Hills lavas (Willcox et al. 2015), and the combined Sr-Nd-Hf isotopic compositions overlap the field of southern African Group-1 kimberlites, which is suggestive of magma derivation from a moderately depleted convecting upper mantle source (Tappe et al. 2020).

Although seismic tomography studies image lower mantle plumes beneath eastern Africa (e.g., Nyblade et al. 2000; Weeraratne et al. 2003), kimberlite melt origins from such thermally anomalous mantle domains is highly unlikely (Stamm and Schmidt 2017; Tappe et al. 2018; Massuyeau et al., 2021), which is supported by a lack of ^{182}W anomalies in the Igwisi Hills kimberlite lavas (Tappe et al. 2020). Mitchell (2008) argued for differentiation of the Igwisi Hills lavas including marked crustal assimilation processes. However, the new isotope data discussed in Tappe et al. (2020) do not support significant crustal contamination.

Samples and analytical techniques

Five polished petrographic thin sections (IH45, IH47, IH53, IH57A, IH57B) were prepared from representative samples of the Igwisi Hills kimberlite lava flows sourced by the NE volcano (see Brown et al. 2012 for detailed field descriptions) (Fig. 1). The petrographic analysis and photomicrograph imaging were done on an Olympus BX51 polarizing microscope at the University of Johannesburg, South Africa. Preferred crystal orientations for two dunitic nodules (IH57BG1 and IH57BG2) were measured by electron backscatter diffraction (EBSD). The EBSD data were collected on a JEOL SEM 6610-LV scanning electron microscope (SEM) installed at the Institute for Mineralogy at the University of Münster, Germany. The SEM instrument is equipped with a LaB_6 electron source plus an Oxford Nordlys EBSD camera running the Oxford HKL Channel-5 software (Version 5.10.50315). We applied a beam current of ~1.5 nA, measured on a retractable Faraday cup, and an accelerating voltage of 20 kV. Working distance was adjusted to 20 mm. EBSD patterns were recorded by the Oxford Flamenco acquisition software and indexing was done using Oxford Tango and Mambo software packages. Detailed descriptions of the EBSD technique employed in Münster can be found in Mukai et al. (2014) and Pabich et al. (2020).

The major element compositions of olivine were determined using a four-WDS spectrometer enabled CAMECA SX100 electron microprobe (EPMA) at the University of Johannesburg. The setup for the measurements was 20 nA electron beam current, 20 kV accelerating voltage, and a beam size of 1 µm. High-resolution backscatter electron (BSE) images were created with the same instrument to study textural features in greater detail and to identify compositional heterogeneity within the dunitic nodules. For a representative number of olivine grains, we conducted X-ray mapping of the areal distributions of Fe, Mg, Ni, Ca, Al and P using a JEOL 8530F electron microprobe with a field emission source at the University of Münster. The analytical conditions were 15 kV accelerating voltage, 2 µm beam size, 80 ms dwell time per pixel, and probe current of 75 nA for major elements and 150 nA for minor elements.

Olivine minor and trace element concentrations were measured by laser ablation inductively coupled plasma mass spectrometry (LA-ICP-MS) at the University of Johannesburg. The instrument setup consists of a 193 nm ArF RESOlution SE155 excimer laser coupled to a Thermo Scientific iCAP RQ ICP-MS instrument. The olivine trace element analytical protocol, including the choice of reference materials and setup of data reduction routines, are reported in detail by Ngwenya and Tappe (2021). Because olivine crystals in incompatible trace element enriched igneous rocks are prone to contamination along cracks (Foley et al. 2011; Rooney et al., 2020), Ngwenya and Tappe (2021) suggested careful screening of olivine analyses with >0.5 ppm Ba and Sr. In this present study of Igwisi Hills olivine macrocrysts and dunitic nodules, we tolerated Ba and Sr contents of up to 2 ppm and 1 ppm, respectively. For magmatic olivine, we tolerated slightly higher Ba and Sr contents of up to 8 ppm and 2 ppm, respectively. MongOl Sh11-2 olivine was analyzed repeatedly as a secondary matrix-matched reference material to monitor data accuracy and precision (Batanova et al. 2019), and to enable corrections of the measured Mn and Sc concentrations. The complete olivine major and trace element dataset for samples and standards is listed in Supp. Table S1, together with the recommended values for standards. Further analytical details can be found in Appendix 1.

Results

Petrography of the kimberlite lavas and included dunitic nodules

The samples of fresh Igwisi Hills kimberlite lavas show an inequigranular texture with abundant anhedral to rounded olivine macrocrysts up to 7 mm across and <2 mm large subhedral-to-euhedral olivine phenocrysts. Abundant rounded to subrounded polycrystalline dunitic nodules (~1–5 mm) and calcite laths (<0.5 mm) also occur. These larger crystals and crystal aggregates are set in a fine-grained carbonate- and chlorite-dominated groundmass. Other groundmass phases identified include abundant irregular fragments of olivine (<0.1 mm), spinel-group minerals, apatite, perovskite and barite. Olivine in the kimberlite lava samples from Igwisi Hills is remarkably fresh, with only little or no serpentinization. Some of the samples show strongly oriented calcite laths and trails of glass pockets in the groundmass indicative of flow alignment in the lava (Fig. 2a-b). Detailed descriptions of the petrography of the Igwisi Hills kimberlites are given by Dawson (1994), Brown et al. (2012) and Willcox et al. (2015). Below we focus on olivine and in particular on the dunitic nodules, which are the subject of this study.

The dunitic nodules typically comprise single or multiple anhedral host olivine crystals that are accompanied by recrystallized anhedral and subhedral neoblasts (Fig. 2c-f). Whereas the host olivine crystals in the dunitic nodules and the discrete olivine macrocrysts show deformation features, such as undulose extinction and kink bands, the neoblasts are undeformed (Fig. 2c-f). There are some notable differences between the dunitic nodules from the Igwisi Hills kimberlites studied here and those from West Greenland aillikites at Kangamiut studied by Arndt et al. (2010). For example, in the Kangamiut aillikites there is a variation of the size of dunitic fragments at fairly similar morphologies, whereas the dunitic nodules from the Igwisi Hills kimberlites are very well rounded and range from elliptical to almost spherical shapes (Fig. 2a, b). Also, the Kangamiut aillikites lack a population of small subrounded olivine grains but they contain abundant euhedral olivine crystals instead, which may represent phenocrysts or disaggregated neoblasts from the larger dunitic nodules (Arndt et al. 2010). We note further that olivine neoblasts in the dunitic nodules from the Igwisi Hills kimberlites tend to occur in clusters of randomly oriented crystals (Fig. 2c, 3b), although some weak alignment of neoblasts may occur along the nodule margins and also at the boundaries between larger host olivine grains (Fig. 2d, e). Single or smaller groups of olivine neoblasts have also been observed within larger host olivine grains (Fig. 2f), a feature that is commonly observed in sheared peridotite xenoliths from the lower cratonic mantle lithosphere (Tappe et al. 2021).

For the Igwisi Hills kimberlites, a magmatic olivine population was identified as phenocrysts and rims on symmetrical olivine crystals based on the presence of Cr-spinel inclusions, which are typically aligned along planar growth faces of the olivine (Fig. 3c). The host olivine crystals of the dunitic nodules studied contain rare inclusions of Cr-pyrope garnet (Fig. 8b) and Cr-rich phlogopite (Fig. 7). Some olivine macrocrysts contain rare inclusions of clinopyroxene and orthopyroxene (Supp. Table 1S).

Olivine major and trace element compositions

The olivine grains in the Igwisi Hills lavas are complexly zoned with homogeneous cores and zoned rims (Supp. Table S1), which is typical for olivine in kimberlites and related rocks from localities worldwide (Mitchell 1986; Tappe et al. 2006; Kamenetsky et al. 2008; Brett et al. 2009; Arndt et al. 2010; Pilbeam et al. 2013; Bussweiler et al. 2015; Howarth and Taylor 2016; Jaques and Foley 2018; Shaikh et al. 2019; Rooney et al. 2020). The cores of host olivine crystals in dunitic nodules and of discrete macrocrysts analyzed here are characterized by elevated forsterite contents (Fo = 89.5–92.4) and high NiO concentrations (0.34–0.46 wt.%) at <0.2 wt.% CaO (Fig. 4a-b), which is typical for cratonic mantle-derived olivine xenocrysts (Kamenetsky et al. 2008; Brett et al. 2009; Sobolev et al. 2009; Tappe et al. 2009; Arndt et al. 2010; Foley et al. 2013). Olivine cores show low concentrations of Al (15–109 ppm), Ti (42–158 ppm), Cr (43–325 ppm) and Mn (617–957 ppm), and extremely low concentrations of Li (<3 ppm) and Cu (<7 ppm) (Supp. Table S1; Fig. 5, 9), which indicates derivation from relatively depleted mantle peridotites (Seitz and Woodland 2000; De Hoog et al. 2010; Ngwenya and Tappe 2021). Olivine neoblasts in the dunitic nodules exhibit a highly restricted range of Fo values (89.6–91.0), which overlap with those values that define the lower end of the Fo range of olivine cores and host olivine crystals in the dunitic nodules (Fig. 4a). The olivine neoblasts show elevated concentrations of Ca, Mn, Al, Sc, Zr, Zn, Gd and Ce compared to the cores of olivine macrocysts and host olivine crystals in dunitic nodules (Fig. 5; Supp. Table 1s). In general, the olivine neoblasts in each dunitic nodule analyzed show a clear enrichment in Fe and incompatible trace elements compared to their host olivine grains (see the element maps in Fig. 6, 7). Olivine phenocrysts and the inner zones of olivine macrocrysts exhibit moderately high Fo contents (89.0–91.2) and an extremely wide range of NiO between 0.09–0.52 wt.%, whereas the rims show narrower ranges of Fo (89.7–91.2) and NiO (0.13–0.34 wt.%) at relatively high trace element concentration levels (e.g., Ca, Ti, Zn, Sc) (Supp. Table S1). In forsterite–NiO space, the olivine rims show a concave-up evolutionary trend typical of olivine fractional crystallization (Gordeychik et al. 2020).

Electron backscatter diffraction (EBSD) and EPMA elemental mapping of olivine

Two dunitic nodules (IH57BG1 and IH57BG2) were selected for EBSD and EPMA elemental mapping (Mg, Fe, Ni, Ca, P). The ~2.5 mm large subrounded IH57BG1 nodule consists of multiple strained host olivine grains and five undeformed olivine neoblasts that occur along fractures and host olivine grain boundaries (Fig. 6). Deformation features in the host olivine grains, such as kink and dislocation bands, are visible in crystallographic orientation maps (Fig. 7). The ~3 mm large IH57BG2 nodule consists of a strained host olivine grain that encloses four discrete undeformed olivine neoblasts (Fig. 7). Grain boundaries between subhedral neoblasts and the host olivine grain are generally straight and rarely curved to bulgy, whereas 'touching' subhedral neoblasts have straight grain boundaries. Grain boundaries between anhedral olivine crystals are commonly curved to irregular. Curved to bulging grain boundaries are indicative of grain boundary migration (Drury and Urai 1990). The two dunitic nodules studied in detail host numerous carbonate-rich melt inclusions ranging in size from <10 µm to up to 250 µm.

The EBSD measurements show that the host olivine grains in the dunitic nodules exhibit crystal-preferred orientations, which suggests a significant contribution of dislocation creep to the deformation mechanism (Fig. 6-7). However, the orientation of the host olivine crystals differs between the two nodules studied within the same thin section. For example, the host olivine crystals in IH57BG1 show slightly diffuse [010] and [001] axes that fall at a high angle (Fig. 6), whereas the distribution of the [100] axis is more concentrated than for the [001] axis in the host olivine grain from dunitic nodule IH57BG2. This may indicate the presence of dominant tilt walls with [100] as the main glide direction. Olivine neoblasts in both nodules show a highly disordered orientation that is strongly dispersed by comparison to their deformed host olivine grains (Fig. 6-7). A similar observation was made for olivine in dunitic nodules from an aillikite dyke of the Kangamiut area in West Greenland (Arndt et al. 2010).

Mapping of the Mg, Fe, Ni and Ca distributions within the two dunitic nodules for which EBSD data had been collected displays three main zones; that is, a highly resorbed core and an inner zone plus a rim. For IH57BG2, the core has a Fo content of ~92.5 and is mantled by a relatively Fe-rich inner zone with a Fo content of ~89. This inner zone contains inclusions of Cr-rich phlogopite, plus numerous minute spinel crystals. The inner zone occupies most of the neoblast area and is overgrown by a relatively Mg-rich rim with a Fo content of ~90. The rim truncates the olivine neoblast, which establishes neoblast formation before the final phase of olivine rim development in the dunitic nodules (Fig. 7). The major and minor element heterogeneity observed in the dunitic nodules is largely independent of crystal orientation as mapped by EBSD analysis. For example, the inner zones of olivine within the IH57BG2 nodule show similar crystallographic orientations compared to the cores of the host olivine grains, but all olivine neoblasts exhibit different orientations. Also, the rims do not have independent orientations but show similar orientations to the olivine cores and neoblasts upon which they grew.

Melt inclusions and fractures in olivine

Both dunitic nodules and olivine macrocrysts exhibit fractures of multiple generations. Fractures of a first-generation tend to be larger and are typically filled with carbonate-rich melt (now glass) plus oxide minerals (Fig. 3a). These early-stage fractures resemble ‘sealed’ cracks (Brett et al. 2015), which run across olivine cores and mostly terminate at core–rim boundaries. Fractures of a second-generation are ‘healed’ cracks (Brett et al. 2015) with a diffuse appearance. They typically contain trails of minute melt/fluid and oxide mineral inclusions (Fig. 3a). The third generation of fractures comprises multiple curvilinear cracks that are restricted to the olivine grain margins (Fig. 2f, 3a, d). In general, fractures propagate from the recrystallized olivine grains (i.e., neoblasts) into host olivine domains (Fig. 3b).

Up to 2 mm large carbonate-rich melt inclusions occur within many olivine grains of the dunitic nodules from the Igwisi Hills kimberlite lavas. The melt inclusions appear to be associated with the inner zones (Fig. 7, 8), and they have irregular to lenticular shapes (Fig. 3a). The melt inclusions are similar to so-called ‘polymineralic’ inclusions commonly observed in kimberlite-borne megacrysts from localities worldwide (Bussweiler, 2019), including megacrystic olivine (Howarth and Büttner 2019; Abersteiner et al. 2019). Another important feature of the Igwisi Hills kimberlite lavas is the presence of quenched carbonate-rich melt pockets in the groundmass. These 50–

400 µm long worm-shaped melt pockets are aligned within the magmatic flow texture (Fig. 2a, b). Alternatively, they may represent 'sheared' vesicles filled with secondary carbonate.

Discussion

Some remarks on the term 'nodule', as used in kimberlite petrology

Arndt and co-workers suggested that all subrounded to rounded mm-sized olivine grains in kimberlites should be referred to as 'dunitic nodules' (Arndt et al. 2010, 2021; Cordier et al. 2015), a view that we find problematic for the following reasons: (i) The rounding of olivine grains does not necessarily reflect petrogenetic processes sensu stricto but is mainly a function of physical processes, such as abrasion and attrition, that operate during fast and turbulent kimberlite magma ascent (Brett et al. 2009, 2015; Moss et al. 2010; Jones et al. 2014). For the same reason, other mantle-derived minerals and mineral aggregates can also attain nodule-like morphologies, for example the oval to round 'glimmerite nodules' in type aillikite from Labrador (Tappe et al. 2006). The roundness of grains is also influenced by other factors such as their depths of origin within the lithospheric mantle (Bussweiler et al. 2015), or the timing of their liberation from mantle-derived xenoliths during magma ascent. (ii) Although Arndt and co-workers stressed that the term 'nodule' is used in a purely descriptive sense without genetic connotations, the meaning is easily confused with that of the term 'microxenolith', which is also problematic for single discrete olivine grains (e.g., Giuliani and Foley 2016). Note further that the term 'macrocryst' is also widely used as a non-genetic descriptor of single grains in kimberlites, and we maintain that 'macrocrysts' and 'nodules' are not necessarily equivalent in terms of their anatomies as well as origins. Here, we suggest the following guidelines as to how such kimberlite petrology jargon could be effectively applied, with special reference to olivine (e.g., Mitchell 1986):

- Single discrete grains between 0.5-10 mm in size = **'macrocrysts'**
- Single discrete grains >10 mm in size = **'megacrysts'**

- Millimeter-sized polycrystalline–monomineralic aggregates = **‘nodules’**
- Millimeter-sized polycrystalline–polymineralic aggregates = **‘microxenoliths’**

(iii) The cores of olivine macrocrysts typically represent mantle-derived xenocrysts, although some cores may be a product of mantle metasomatism (Howarth and Taylor 2016) or mantle source ‘defertilization’ (Arndt et al. 2010). Hence, there are olivine macrocryst populations in kimberlites and related rocks that have no apparent relationship to dunitic nodules, such that it is inaccurate to label all rounded olivine grains as ‘nodules’. (iv) Many kimberlites, including those from the Igwisi Hills, contain large amounts of highly complex rounded to subrounded olivine grains that cannot be linked to a single lithospheric mantle source or metasomatic process (see the discussion below). Therefore, it is not warranted to consider sizable discrete olivine grains without any recrystallized subgrains as ‘nodules’, and we opt for such single olivine crystals to be referred to as ‘macrocrysts’, as exemplified by the following petrogenetic discussion.

Origins of dunitic nodules and their significance for kimberlite petrogenesis

Constraints from the host olivine grains of dunitic nodules

Previous models suggested that dunitic nodules in hypabyssal kimberlites and related rocks are sourced from peridotites at the base of cratonic mantle lithosphere (e.g., Arndt et al. 2010; Cordier et al. 2015; Rooney et al. 2020), which appears to be metasomatically overprinted by proto-kimberlitic melts. During mantle metasomatism, olivine can attain more Fe-rich compositions (Howarth and Taylor 2016; Shaikh et al. 2019), with or without preserved olivine relicts that are Mg-rich. Several dunitic nodules from the Igwisi Hills kimberlite lavas preserve Mg-rich host olivine crystals, and their core compositions are similar to olivine in refractory cratonic mantle peridotites (Fig. 4a, b). These ‘inherited’ relicts from peridotite-dominated cratonic mantle lithosphere can be used to extract information about the origin of olivine crystal cargo in kimberlites and related rocks (Bussweiler et al. 2017; Jaques and Foley

2018; Shaikh et al. 2019; Ngwenya and Tappe 2021). Relict olivine cores in the dunitic nodules (e.g., IH53N1, IH47G1, IH57AG1, IH57AG2) have similar major and trace element compositions to olivine in coarse granular peridotite xenoliths recovered from kimberlites on all major cratons (Fig. 4a, b). Their Mn/Al, Zr/Sc and V/Al systematics suggest garnet-facies peridotites as the source (Fig. 9a, b), which is supported by the presence of garnet inclusions inside the host olivine domains of the dunitic nodules (Fig. 7).

Relict olivine cores of the dunitic nodules and the cores of discrete olivine macrocrysts derived from garnet-bearing peridotites (Fig. 9a, b) can be used to calculate Al-in-olivine temperatures applying the calibration of Bussweiler et al. (2017). Olivine equilibration temperatures were calculated for assumed pressures of 40, 50, 60 and 70 kbar; i.e., a pressure range equivalent to ~130-230 km depth. By using iterative calculations, the obtained Al-in-olivine temperatures were then projected onto the Cenozoic geotherm of the Tanzania craton at ~41 mW/m^2 (Gibson et al. 2013). Such data treatment yields information about the approximate vertical distribution of peridotite-derived olivine within the cratonic mantle column (Fig. 10). The projected temperature solutions reveal a lithosphere thickness of ~180 km, with a kimberlite magma sampling interval between 100–160 km depth. These data also suggest a ~50 km thick diamond window beneath the Igwisi Hills consistent with previous P-T constraints for the Tanzania craton during Cenozoic times (Gibson et al. 2013).

Our petrology-based estimate of the lithosphere thickness is consistent with the majority of geophysical studies that indicate a ~180 km thick lithosphere beneath the central part of the Tanzania craton (Ritsema et al. 1998; Nyblade et al. 2000; Weeraratne et al. 2003; Tiberi et al. 2019; Clutier et al. 2021), although Globig et al. (2016) suggest a thinner cratonic lithosphere of ~150-160 km thickness for the study region. Given that peridotitic mantle xenoliths from Labait volcano, located at the rifted eastern margin of the Tanzania craton, record a maximum depth of origin of ~150 km (Lee and Rudnick 1999), a ~180 km thick continental lithosphere beneath the central and western parts of the craton, more distal to the strong influence of the East African Rift, appears to be reasonable.

Our P-T estimates for the relict olivine cores of the dunitic nodules (850-1126 ºC and 32-46 kbar) suggest an origin from between 100 and 145 km depth (Fig. 10). This implies entrainment of peridotitic material by the rising kimberlite magmas along roughly 1/3rd of the mantle lithosphere column from near the craton base to mid-lithospheric depth. Hence, dunitic nodule formation is not restricted to the craton base, as was assumed in previous models for kimberlite petrogenesis (Arndt et al. 2010; Cordier et al. 2015). Our results suggest that a major portion of the lower lithospheric mantle column is involved in fluid/melt-assisted recrystallization processes and metasomatic reactions along kimberlite magma conduits, and these mechanisms would certainly influence the major element compositions of ascending kimberlite melts, as had been suggested in previous studies (Mitchell 2008; Kjarsgaard et al. 2009; Russell et al. 2012; Pilbeam et al. 2013; Soltys et al. 2016; Dongre and Tappe 2019; Giuliani et al. 2020; Dalton et al. 2020; Tovey et al. 2021). The ascent of highly reactive and progressively evolving kimberlitic to carbonatitic melts has been argued to produce a wide range of metasomatic imprints on the lower half of the cratonic mantle lithosphere (e.g., Tappe et al. 2011, 2017; Giuliani et al. 2013; Kargin et al. 2016; Fitzpayne et al. 2019; Kopylova et al. 2021). This finding is also consistent with many cratonic mantle peridotite xenolith studies that showed fluid/melt-assisted recrystallization features over several 10s of kilometers thick depth ranges (Drury and van Roermund 1989; Tommasi et al. 2008; Baptiste et al. 2012; Tappe et al. 2021). This form of reactive melt transport may equate to the 'defertilization' process invoked by Arndt et al. (2010) for the origin of dunitic nodules in kimberlites and related rocks, although the rather passive role of olivine in this model has been challenged (Giuliani and Foley 2016; Moore 2017; Rooney et al. 2020).

Constraints from olivine neoblasts in the dunitic nodules

On the basis of morphology, two types of olivine neoblasts, namely anhedral and subhedral-to-euhedral crystals, are identified in the dunitic nodules from the Igwisi Hills kimberlites, and elsewhere. The subhedral-to-euhedral neoblasts are commonly referred to as 'tablets' (e.g., Arndt et al. 2010). Here, we emphasize that both types of neoblasts may be genetically linked, and possibly formed during different stages in the evolution of kimberlite magmas. The anhedral olivine neoblasts are thought to form by fluid/melt-assisted recrystallization and annealing of mantle peridotites shortly after plastic deformation such as shearing (Drury and van Roermund 1989). With further stress-release, the anhedral olivine neoblasts may grow into euhedral tablets by static re-equilibration and annealing (Boullier and Nicolas 1975; Guéguen 1977; Mercier 1979; Green and Guéguen 1983), possibly during ascent of the kimberlite magma and its entrained mantle cargo (Mercier 1979; Green and Guéguen 1983; Arndt et al. 2010). In our samples from Igwisi Hills, a progressive olivine recrystallization mechanism is supported by the fact that both neoblast types co-exist in the same nodule, suggesting a genetic association (Fig. 2c, e). Furthermore, crystallographic orientation maps advocate random growth of the olivine neoblasts in an environment of lower strain relative to sheared mantle lithosphere, such as rising magmas (Fig. 6, 7).

Several dunitic nodules show distributions of multiple cracks propagating from recrystallized grains into host olivine domains (Fig. 3c). Crack propagation was probably driven by fluid/melt percolation and decompression during magma ascent (Jones et al. 2014; Bussweiler et al. 2016). These textural observations suggest that at least some of the fractures formed during recrystallization processes. Hence, fluid/melt-assisted recrystallization weakens peridotitic mantle rocks mainly by increasing the number and length of olivine grain boundaries and also by creating additional fractures (Drury and van Roermund 1989), which altogether promotes disaggregation of mantle cargo in ascending kimberlite magmas. This idea is supported by the presence of olivine neoblasts that tend to be aligned along fractures in the dunitic nodules (Fig. 2e).

Constraints from the ‘inner zones’ of olivine grains

So-called ‘inner zones’ of olivine are reported from magmatic kimberlites and related rocks worldwide (Fedortchouk and Canil 2004; Kamenetsky et al. 2008; Pilbeam et al. 2013; Bussweiler et al. 2015; Cordier et al. 2015; Howarth and Taylor 2016; Giuliani 2018; Lim et al. 2018; Soltys et al. 2018, 2020; Shaikh et al. 2019; Tovey et al. 2020).

Their formation has been variably explained by: (i) solid-state diffusion (Pilbeam et al. 2013), (ii) equilibration between olivine cores and interacting proto-kimberlite melts (Cordier et al. 2015; Howarth and Taylor 2016), and (iii) a direct overgrowth of olivine cores by host kimberlite magmas (Pilbeam et al. 2013; Howarth and Taylor 2016; Soltys et al. 2018). In this paper, we do not discuss the complex compositional trends of the 'inner zones' of olivine in kimberlites, because this topic has been covered extensively by Cordier et al. (2015), Giuliani (2018), Lim et al. (2018) and Soltys et al. (2020), to name a few studies. Instead, we focus on the timing of 'inner zone' formation with respect to the various known main stages of kimberlite magma evolution.

The inner zones of olivine grains from the Igwisi Hills kimberlite lavas typically have a gradational border with the core zones (Fig. 6, 7, 8), but sharp contacts have been observed for a few grains (Fig. 8c). A key observation of this study is that olivine-hosted melt inclusions and olivine neoblasts are associated exclusively with such 'inner zones' (Fig. 8a-d). The smallest melt inclusions form trails and correspond to healed cracks, whereas larger inclusions resemble sealed cracks (Brett et al. 2015). It appears that the liquid trapped in these inclusions was involved in fluid/melt-assisted recrystallization processes, including metasomatic enrichment of mantle-derived olivine, which possibly gave rise to the inner zones. The melt inclusions have a carbonate-rich character consistent with some of the proposed compositions of proto-kimberlite melt (Kamenetsky et al. 2008; Giuliani et al. 2012; Russell et al. 2012; Pilbeam et al. 2013; Brett et al. 2015; Bussweiler et al. 2016; Soltys et al. 2016), which is argued to be ubiquitous near the cratonic lithosphere-asthenosphere boundary (Gregoire et al. 2006; Tappe et al. 2018). The inner zones of some olivine grains exhibit trails of spinel inclusions near the contact with the olivine cores (Fig. 8b). Combined, these features suggest that the inner zones of some olivine grains formed by direct crystallization from kimberlitic magma, whereas in other grains they may represent equilibration zones that formed by the interaction between olivine cores and host magma. Indeed, the inner zones analyzed are enriched in Ni, Ca and Mn (Fig. 6, 7), and they have Fo contents that are very similar to those of the olivine phenocrysts (Fig. 4), which supports a genetic link to kimberlitic magma.

Howarth and Taylor (2016) suggested that some of the inner zones (their 'melt zones') of olivine grains formed by direct crystallization from kimberlitic magma and may thus represent equilibration zones, as also noted by other authors (Arndt et al. 2010; Kamenetsky et al. 2008). Cordier et al. (2015) introduced the term 'grain boundary zone' for inner zones of olivine grains in dunitic nodules, which largely corresponds to 'equilibration zones'. Irrespective of nomenclature, equilibration zones occur mainly as: (i) a continuous rim sandwiched between olivine core and overgrowth rim (e.g., Fig. 7, 8d), and (ii) a marginal zone along grain boundaries and fractures in dunitic nodules and discrete olivine macrocrysts (e.g., Fig. 6). The first type of equilibration zone occurs in the majority of discrete olivine macrocrysts and dunitic nodules, where they are continuous and typically show evidence of resorption before the formation of overgrowth rims (Fig. 7, 8d, 11a). From these textures, it can be inferred that thin melt films 'wetted' entire olivine grains within peridotitic mantle domains (e.g., Drury and van Roermund 1989). Thus, these zones may record the onset of melt accumulation at the base of cratonic lithosphere, possibly shortly prior to kimberlite magma eruptions (Cordier et al. 2015). We note that several olivine macrocrysts exhibit discontinuous equilibration zones as illustrated in Figure 11b. In these grains, olivine cores may show a sharp yet discontinuous contact with the overgrowth rims indicating that equilibration zones did not develop fully around an entire olivine core zone. In this case, equilibration zones must have formed before breakage or liberation of the olivine crystal from its parent xenolith or a larger xenocryst. In kimberlite-borne dunitic nodules, the most common equilibration zones in olivine occur along grain boundaries, which provide ample open volume for percolating melts (Faul 1997).

Links to megacryst formation

A link between Fe-rich olivine cores of metasomatic origin and megacryst suites (i.e., large discrete crystals of olivine, garnet, clinopyroxene, orthopyroxene, ilmenite, zircon and phlogopite) had been proposed by Moore and Costin (2016) based on major and minor element compositions. Giuliani and Foley (2016) and Moore (2017) pointed out that Fe-rich dunitic nodules in kimberlites could be sourced from olivine megacrysts because of their strong compositional similarities. Similar to the proposed origin of the dunitic nodule suite (e.g., Arndt et al. 2010), megacryst formation is widely attributed to interactions between proto-kimberlite melt and cratonic mantle lithosphere (Hops et al. 1992; Nowell et al. 2004; Moore and Belousova 2005; Kopylova et al. 2009; Tappe et al. 2011; Giuliani et al. 2013; Kargin et al. 2016; Bussweiler et al. 2018; Sun et al. 2018), which involves the growth of large crystals (1–15 cm) coupled to strong plastic deformation and recrystallization processes (e.g., Tappe et al., 2021, and references therein).

The Igwisi Hills kimberlite lavas lack extremely Fe-rich olivine compositions with Fo <88, which are known from many kimberlites on major cratons worldwide (Giuliani 2018). However, several Igwisi Hills olivine populations, including the neoblasts and inner zones, show moderate Fe-enrichment with Fo <91, which is similar to olivine in sheared cratonic peridotite xenoliths (Fo ~86–92; Fig. 4) (Hervig et al. 1986; Tappe et al. 2021), but still higher than Fo 82-88 as typically reported for olivine megacrysts in kimberlites (Moore and Costin 2016; Howarth 2018). Links between olivine megacrysts and dunitic nodules in kimberlites are supported by their elevated concentrations of Ca, Mn, Al, Sc and V (Fig. 5, 9). Also, similar sizes and textures of olivine grains are noted for dunitic nodules and discrete megacrysts in kimberlites and related rocks, further establishing a possible genetic relationship between these olivine types (Arndt et al. 2021). Iron and trace element enrichment in olivine has been linked to melt-related metasomatism of peridotitic mantle wall-rocks (e.g., Howarth and Taylor 2016). Thus, the lack of strong Fe-enrichment in olivine from the Igwisi Hills kimberlite lavas suggests a rather limited extent of enrichment of their source rocks in the lithospheric mantle beneath this part of the Tanzania craton, which is consistent with the paucity of Fe-enriched olivine in mantle-derived peridotite xenoliths and diamonds from the study region (Dawson 1994; Stachel et al. 1998; Gibson et al. 2013).

In contrast to the original models of megacryst formation, in which these large crystals were envisaged to form from melts pooled at the lithosphere–asthenosphere boundary (e.g., Nixon and Boyd 1973), newer research demonstrates much longer depth ranges for the formation of megacrysts within the cratonic mantle lithosphere (Giuliani et al. 2013; Kargin et al. 2016; Bussweiler et al. 2018; Tappe et al. 2021). A wide range of Ni-in-garnet temperatures is typically recorded by megacrystic garnet grains recovered from kimberlites on all major cratons (e.g., Griffin et al. 2002; Kobussen et al. 2008; Hunt et al. 2012; Shaikh et al. 2020), which additionally supports long depth ranges for megacryst formation and, by extension, long depth ranges for the formation of dunitic nodules, as is demonstrated here.

Where and when does mantle-derived olivine deform?

Olivine deformation features, such as kink banding and undulose extinction, are often ascribed to strain within the lithospheric mantle, and their identification is typically used as evidence for a xenocrystic origin of olivine in mantle-derived magmatic rocks (Skinner 1989; Tappe et al. 2009; Cordier et al. 2015). This concept has been contested by Moore et al. (2020), who proposed that olivine grains in kimberlites may have been deformed at crustal levels, with the implication that deformation features alone do not provide unequivocal evidence for a xenocrystic origin from the cratonic mantle. A similar line of evidence was developed earlier by Kresten (1973), Moore (1988, 2012) and Shaikh et al. (2018), in which deformation of olivine phenocrysts was ascribed to torsional forces applied to the kimberlite magma during ascent.

The Igwisi Hills kimberlite samples show a peculiar textural feature that developed on rounded olivine macrocrysts. These olivine crystals show curvilinear fractures that run parallel within the curved grain margins (Fig. 3a). Such curvilinear fractures were also reported by Jones et al. (2014), who ascribed them to the relief from internal forces due to ascent-driven magma decompression. However, the parallel nature of these tangentially oriented fractures seems to indicate external stresses caused by rotation of the olivine crystals during turbulent transport along kimberlite magma conduits. Importantly, undulose extinction has been observed in this type of rounded olivine crystal, propagating into the grain interiors. Hence, it is evident indeed that besides ubiquitous deformation of olivine within the lithospheric mantle, magmatic olivine grains also deform in response to appreciable forces during magma transport, even at crustal levels. We note, however, that olivine in kimberlites and related rocks exhibits most commonly mantle-derived deformation features and that the much rarer deformation attained during magma ascent can be readily identified within olivine overgrowth rims.

Conclusions

Dunitic nodules from the Quaternary Igwisi Hills kimberlite volcanoes were studied for their petrography, olivine major and trace element compositions, and olivine crystallographic orientations. Host olivine grains in the dunitic nodules yielded a wide range of Al-in-olivine temperatures, which translates after regional geotherm projections into a sampling interval between 100 and 145 km depth. An origin of the dunitic nodules from mid-lithospheric depths is in contrast to previous models, in which these olivine-dominated materials were assumed to form exclusively at the base of cratonic mantle lithosphere by metasomatic processes that lead-up to kimberlite magma ascent and eruptions.

Our data show that melt/fluid-assisted recrystallization of olivine and its concomitant metasomatic enrichment are common processes that operate along kimberlite magma conduits within the lower half of typical cratonic mantle lithosphere. We demonstrate that equilibration zones in mantle-derived olivine crystals can form by mineral–melt interactions at the base of cratonic lithosphere, but also along translithospheric kimberlite magma conduit systems. It appears that the petrogenesis of dunitic nodules in kimberlites shares many characteristics with the formation of olivine megacrysts, and both these olivine types may represent a product of strong interactions between asthenosphere-derived carbonate-rich melts and lithospheric mantle rocks.

Acknowledgements

AMS acknowledges the University of Johannesburg for providing a postdoctoral fellowship, which was financially supported through DSI-NRF SARChI funds awarded to Fanus Viljoen and a Faculty of Science award to ST. ST acknowledges additional financial support by the DSI-NRF CIMERA Centre of Excellence and the Geological Society of South Africa (REI grants 2019-2020). YB was funded through an EU Marie Skłodowska-Curie Fellowship (Project ID 746518) and acknowledges subsequent funding through a University of Münster postdoctoral scholarship. RJB acknowledges a National Geographic Committee on Research and Exploration grant (No. 8562-08). Jasper Berndt is sincerely thanked for running the X-ray element maps in Münster. Christian Reinke and Henriette Ueckermann are gratefully acknowledged for technical support during the EPMA and LA-ICP-MS analytical work in Johannesburg. The journal reviewers Nick Arndt and Andrea Giuliani are gratefully acknowledged for their highly constructive comments on and critique of our initial manuscript version. Hans Keppler is sincerely thanked for his consummate editorial handling.

References

Abersteiner A, Kamenetsky VS, Goemann K, et al (2019) Polymineralic inclusions in kimberlite-hosted megacrysts: Implications for kimberlite melt evolution. Lithos 336–337:310–325. doi: https://doi.org/10.1016/j.lithos.2019.04.004

Arndt NT, Cordier C, Boullier A, et al (2021) Olivine in kimberlites – macrocrysts, megacrysts and dunitic nodules, all from a single source. *In preparation.*

Arndt NT, Guitreau M, Boullier A, et al (2010) Olivine, and the Origin of Kimberlite. J Petrol 51:573–602. doi: 10.1093/petrology/egp080

Baptiste V, Tommasi A, Demouchy S (2012) Deformation and hydration of the lithospheric mantle beneath the Kaapvaal craton, South Africa. Lithos 149:31–50

Batanova VG, Thompson JM, Danyushevsky L V., et al (2019) New Olivine Reference Material for In Situ Microanalysis. Geostand Geoanalytical Res 43:453–473. doi: 10.1111/ggr.12266

Bell K, Dodson MH (1981) The geochronology of the Tanzanian shield. J Geo 89:109–128

Boullier AM, Nicolas A (1975) Classification of textures and fabrics of peridotite xenoliths from South African kimberlites. Phy Chem Earth 9:467–475

Brett RC, Russell JK, Andrews GDM, Jones TJ (2015) The ascent of kimberlite: Insights from olivine. Earth Planet Sci Lett 424:119–131. doi: 10.1016/j.epsl.2015.05.024

Brett RC, Russell JK, Moss S (2009) Origin of olivine in kimberlite: Phenocryst or impostor? Lithos 112:201–212. doi: 10.1016/j.lithos.2009.04.030

Brown RJ, Manya S, Buisman I, et al (2012) Eruption of kimberlite magmas: Physical volcanology, geomorphology and age of the youngest kimberlitic volcanoes known on earth (the Upper Pleistocene/Holocene Igwisi Hills volcanoes, Tanzania). Bull. Volcanol. 74:1621–1643

Bussweiler Y (2019) Polymineralic inclusions in megacrysts as proxies for kimberlite melt evolution—a review. Minerals 9:530. doi: 10.3390/min9090530

Bussweiler Y, Brey GP, Pearson DG, et al (2017) The aluminium-in-olivine thermometer for mantle peridotites — Experimental versus empirical calibration and potential applications. Lithos 272–273:301–314. doi: 10.1016/j.lithos.2016.12.015

Bussweiler Y, Foley SF, Prelević D, Jacob DE (2015) The olivine macrocryst problem: New insights from minor and trace element compositions of olivine from Lac de Gras kimberlites, Canada. Lithos 220–223:238–252. doi: 10.1016/j.lithos.2015.02.016

Bussweiler Y, Pearson DG, Stachel T, Kjarsgaard BA (2018) Cr-rich megacrysts of clinopyroxene and garnet from Lac de Gras kimberlites, Slave Craton, Canada – implications for the origin of clinopyroxene and garnet in cratonic lherzolites. Mineral Petrol 112:583–596. doi: 10.1007/s00710-018-0599-2

Bussweiler Y, Stone RS, Pearson DG, et al (2016) The evolution of calcite-bearing kimberlites by melt-rock reaction: evidence from polymineralic inclusions within clinopyroxene and garnet megacrysts from Lac de Gras kimberlites, Canada. Contrib to Mineral Petrol 171:1–25. doi: 10.1007/s00410-016-1275-3

Clutier A, Gautier S, Tiberi C (2021) Hybrid local and teleseismic P-wave tomography in North Tanzania: Role of inherited structures and magmatism on continental rifting. Geophys J Int 224:1588–1606. doi: 10.1093/gji/ggaa538

Cordier C, Sauzeat L, Arndt NT, et al (2015) Metasomatism of the lithospheric mantle immediately precedes kimberlite eruption: New evidence from olivine composition and microstructures. J Petrol 56:1775–1796. doi: 10.1093/petrology/egv054

Dawson JB (1971) Advances in kimberlite geology. Earth Sci Rev 7:187-214

Dawson JB (1994) Quaternary kimberlitic volcanism on the Tanzania Craton. Contrib to Mineral Petrol 116:473–485. doi: 10.1007/BF00310913

Day HW (2012) A revised diamond-graphite transition curve. Am Mineral 97:52–62

De Hoog JCM, Gall L, Cornell DH (2010) Trace-element geochemistry of mantle olivine and application to mantle petrogenesis and geothermobarometry. Chem Geol 270:196–215. doi: 10.1016/j.chemgeo.2009.11.017

Dongre A, Tappe S (2019) Kimberlite and carbonatite dykes within the Premier diatreme root (Cullinan Diamond Mine, South Africa): New insights to mineralogical-genetic classifications and magma CO_2 degassing. Lithos 338–339:155–173. doi: 10.1016/j.lithos.2019.04.020

Drury MR, van Roermund HLM (1989) Fluid assisted recrystallization in upper mantle peridotite xenoliths from kimberlites. J Petrol 30:133–152. doi: 10.1093/petrology/30.1.133

Drury MR, Urai JL (1990) Deformation-related recrystallization processes. Tectonophysics 172:235–253

Faul UH (1997) Permeability of partially molten upper mantle rocks from experiments and percolation theory. J Geophys Res 102:10299-10311

Fedortchouk Y, Canil D (2004) Intensive variables in kimberlite magmas, Lac de Gras, Canada and implications for diamond survival. J Petrol 45:1725–1745. doi: 10.1093/petrology/egh031

Fitzpayne A, Giuliani A, Maas R, et al (2019) Progressive metasomatism of the mantle by kimberlite melts: Sr–Nd–Hf–Pb isotope compositions of MARID and PIC minerals. Earth Planet Sci Lett 509:15–26. doi: 10.1016/j.epsl.2018.12.013

Foley SF, Jacob DE, O'Neill HSC (2011) Trace element variations in olivine phenocrysts from Ugandan potassic rocks as clues to the chemical characteristics of parental magmas. Contrib to Mineral Petrol 162:1–20

Foley SF, Prelevic D, Rehfeldt T, Jacob DE (2013) Minor and trace elements in olivines as probes into early igneous and mantle melting processes. Earth Planet Sci Lett 363:181–191. doi: 10.1016/j.epsl.2012.11.025

Gibson SA, McMahon SC, Day JA, Dawson JB (2013) Highly refractory lithospheric mantle beneath the Tanzanian craton: Evidence from Lashaine pre-metasomatic garnet-bearing peridotites. J Petrol 54:1503–1546. doi: 10.1093/petrology/egt020

Giuliani A, Kamenetsky VS, Kendrick M A, et al (2013) Oxide, sulphide and carbonate minerals in a mantle polymict breccia: Metasomatism by proto-kimberlite magmas, and relationship to the kimberlite megacrystic suite. Chem Geol 353:4–18. doi: 10.1016/j.chemgeo.2012.09.025

Giuliani A (2018) Insights into kimberlite petrogenesis and mantle metasomatism from a review of the compositional zoning of olivine in kimberlites worldwide. Lithos 312–313:322–342. doi: 10.1016/j.lithos.2018.04.029

Giuliani A, Foley SF (2016) The geochemical complexity of kimberlite rocks and their olivine populations: A comment on Cordier et al. (Journal of Petrology, 56, 1775-1796, 2015). J Petrol 57. doi: 10.1093/petrology/egw026

Giuliani A, Graham Pearson D, Soltys A, et al (2020) Kimberlite genesis from a common carbonate-rich primary melt modified by lithospheric mantle assimilation. Sci Adv 6:1–10. doi: 10.1126/sciadv.aaz0424

Giuliani A, Kamenetsky VS, Phillips D, et al (2012) Nature of alkali-carbonate fluids in the sub-continental lithospheric mantle. Geology 40:967–970. doi: 10.1130/G33221.1

Globig J, Fernàndez M, Torne M, et al (2016) New insights into the crust and lithospheric mantle structure of Africa from elevation, geoid, and thermal analysis. J Geophys Res Solid Earth 121:3782–3803. doi: 10.1002/2015JB012608.Received

Gordeychik B, Churikova T, Shea T, et al (2020) Fo and Ni Relations in Olivine Differentiate between Crystallization and Diffusion Trends. J Petrol 61:1–23. doi: 10.1093/petrology/egaa083

Green DH, Falloon TJ (1998) Pyrolite: a Ringwood concept and its current expression. In: Jackson, I. (ed.) The Earth's Mantle. Cambridge: Cambridge University Press, pp 311–378

Green HW (II), Guéguen Y (1983) Deformation of peridotite in the mantle and extraction by kimberlite: a case history documented by fluid and solid precipitates in olivine. Tectonophysics 92:71–92

Gregoire M, Rabinowicz M, Janse AJA (2006) Mantle mush compaction: A key to understand the mechanisms of concentration of kimberlite melts and initiation of swarms of kimberlite dykes. J Petrol 47:631–646

Griffin WL, Fisher NI, Friedman JH, et al (2002) Cr-pyrope garnets in the lithospheric mantle 2. Compositional populations and their distribution in time and space. Geochem Geophys Geosyst 3:1–35

Guéguen Y (1977) Dislocations In mantle peridotite nodules. Tectonophysics 39:231–254

Gurney JJ, Jakob WRO, Dawson JB (1979) Megacrysts from the Monastery Kimberlite Pipe, South Africa. The Mantle Sample: Inclusion in Kimberlites and Other Volcanics pp 227–243

Hasterok D, Chapman DS (2011) Heat production and geotherms for the continental lithosphere. Earth Planet Sci Lett 307:59–70

Hervig RL, Smith JV, Dawson JB (1986) Lherzolite xenoliths in kimberlites and basalts: petrogenetic and crystallochemical significance of some minor and trace elements in olivine, pyroxenes, garnet and spinel. Transactions of the Royal Society of Edinburgh: Earth Sciences 77:181–201

Howarth GH (2018) Olivine megacryst chemistry, Monastery kimberlite: constraints on the mineralogy of the HIMU mantle reservoir in southern Africa. Lithos 314–315:658–668

Howarth GH, Büttner SH (2019) New constraints on archetypal South African kimberlite petrogenesis from quenched glass-rich melt inclusions in olivine megacrysts. Gondwana Res 68:116–126. doi: https://doi.org/10.1016/j.gr.2018.11.009

Howarth GH, Taylor LA (2016) Multi-stage kimberlite evolution tracked in zoned olivine from the Benfontein sill, South Africa. Lithos 262:384–397. doi: 10.1016/j.lithos.2016.07.028

Hunt L, Stachel T, Grütter H et al. (2012) Small mantle fragments from the Renard kimberlites, Quebec: Powerful recorders of mantle lithosphere formation and modification beneath the eastern Superior craton. J Petrol 53:1597–1635

Jaques AL, Foley SF (2018) Insights into the petrogenesis of the West Kimberley lamproites from trace elements in olivine. Mineral Petrol 112:519–537. doi: 10.1007/s00710-018-0612-9

Jones TJ, Russell JK, Porritt LA, Brown RJ (2014) Morphology and surface features of olivine in kimberlite: Implications for ascent processes. Solid Earth 5:313–326. doi: 10.5194/se-5-313-2014

Kamenetsky VS, Kamenetsky MB, Sobolev AV, et al (2008) Olivine in the Udachnaya-East kimberlite (Yakutia, Russia): Types, compositions and origins. J Petrol 49:823–839. doi: 10.1093/petrology/egm033

Kargin AV, Sazonova LV, Nosova AA, Tretyachenko VV (2016) Composition of garnet and clinopyroxene in peridotite xenoliths from the Grib kimberlite pipe, Arkhangelsk diamond province, Russia: Evidence for mantle metasomatism associated with kimberlite melts. Lithos 262:442–455. doi: 10.1016/j.lithos.2016.07.015

Kjarsgaard BA, Pearson DG, Tappe S, et al (2009) Geochemistry of hypabyssal kimberlites from Lac de Gras, Canada: Comparisons to a global database and applications to the parent magma problem. Lithos 112:236–248. doi: 10.1016/j.lithos.2009.06.001

Kobussen AF, Griffin WL, O'Reilly SY, Shee SR (2008) Ghosts of lithospheres past: imaging an evolving lithospheric mantle in southern Africa. Geology 36:515–518

Kopylova MG, Ma F, Tso E (2021) Constraining carbonation freezing and petrography of the carbonated cratonic mantle with natural samples. Lithos 388:1-15

Kopylova MG, Nowell GM, Pearson DG, Markovic G (2009) Crystallization of megacrysts from protokimberlitic fluids : Geochemical evidence from high-Cr megacrysts in the Jericho kimberlite. Lithos 112:284–295. doi: 10.1016/j.lithos.2009.06.008

Kreston P (1973) The geology of Lemphane pipes and neighbouring intrusions. In: Nixon P.H. (ed.) Lesotho kimberlites. Cape and Transvaal Printers, Cape Town, pp 159–167

Lee C-T, Rudnick RL (1999) Compositionally stratified cratonic lithosphere: Petrology and geochemistry of peridotite xenoliths from the Labait Volcano, Tanzania, in Gurney, J.J., Gurney, J.L., Pascoe, M.D., and Richardson, S.H., eds., The P.H. Nixon Volume: Proceedings of the 7th International Kimberlite Conference: Cape Town, Red Roof Design, p. 503–521.

Lim E, Giuliani A, Phillips D, Goemann K (2018) Origin of complex zoning in olivine from diverse, diamondiferous kimberlites and tectonic settings: Ekati (Canada), Alto Paranaiba (Brazil) and Kaalvallei (South Africa). Mineral Petrol 112:539–554. doi: 10.1007/s00710-018-0607-6

Massuyeau M, Gardes E, Rogerie G, et al. (2021). MAGLAB: A computing platform connecting geophysical signatures to melting processes in Earth's mantle. Physics of the Earth and Planetary Interiors 106638

Mercier JXC (1979) Peridotite xenoliths and the dynamics of kimberlite intrusion. In: FR Boyd and HDA Meyer (Editors), The Mantle Sample. American Geophysical Union, Washington, D.C., pp 197–212

Mitchell RH (1970) Kimberlite and Related Rocks: A Critical Reappraisal. J Geol 78:686–704. doi: 10.1086/627571

Mitchell RH (1986) Kimberlites: Mineralogy, Geochemistry, and Petrology

Mitchell RH (2008) Petrology of hypabyssal kimberlites: Relevance to primary magma compositions. J Volcanol Geotherm Res 174:1–8. doi: 10.1016/j.jvolgeores.2007.12.024

Mitchell RH, Giuliani A, O'Brien H (2019) What is a Kimberlite? Petrology and Mineralogy of Hypabyssal Kimberlites. Elements 15:381–386. doi: 10.2138/gselements.15.6.381

Moore A, Belousova E (2005) Crystallization of Cr-poor and Cr-rich megacryst suites from the host kimberlite magma : implications for mantle structure and the generation of kimberlite magmas. Contrib to Mineral Petrol 149:462–481. doi: 10.1007/s00410-005-0663-x

Moore A, Costin G (2016) Kimberlitic olivines derived from the Cr-poor and Cr-rich megacryst suites. Lithos 258–259:215–227. doi: 10.1016/j.lithos.2016.04.022

Moore A, Yudovskaya M, Proyer A, Blenkinsop T (2020) Evidence for olivine deformation in kimberlites and other mantle-derived magmas during crustal emplacement. Contrib to Mineral Petrol 175:1–9. doi: 10.1007/s00410-020-1653-8

Moore AE (1988) Olivine: a monitor of magma evolutionary paths in kimberlites and olivine melilitites. Contrib to Mineral Petrol 99:238–248. doi: 10.1007/BF00371464

Moore AE (2012) The case for a cognate, polybaric origin for kimberlitic olivines. Lithos 128–131:1–10. doi: 10.1016/j.lithos.2011.11.002

Moore AE (2017) Quantitative Modelling of the Apparent Decoupling of Mg # and Ni in Kimberlitic Olivine Margins : Comment on Cordier et al. (Journal of Petrology, 56, 1775-1796, 2015) J Petrol 58:385–390. doi: 10.1093/petrology/egx014

Moss S, Russell JK, Smith BHS, Brett RC (2010) Olivine crystal size distributions in kimberlite. Am Mineral 95:527–536. doi: 10.2138/am.2010.3277

Mukai H, Austrheim H, Putnis CV, Putnis A (2014) Textural evolution of plagioclase feldspar across a shear zone: Implications for deformation mechanism and rock strength. J Petrol 55:1457–1477

Ngwenya NS, Tappe S (2021) Diamondiferous lamproites of the Luangwa Rift in Central Africa and links to remobilized cratonic lithosphere. Chem Geol 120019. doi: https://doi.org/10.1016/j.chemgeo.2020.120019

Nixon PH, Boyd FR (1973) The discrete nodule association in kimberlites from northern Lesotho. In: Lesotho kimberlites. Maseru, Lesotho National Development Corp. Cape and Transvaal Printers, South Africa. 67–75

Nowell GM, Pearson DG, Bell DR, et al (2004) Hf Isotope Systematics of Kimberlites and their Megacrysts: New Constraints on their Source Regions. J Petrol 45:1583–1612. doi: 10.1093/petrology/egh024

Nyblade AA, Owens TJ, Gurrola H, et al (2000) Seismic evidence for a deep upper mantle thermal anomaly beneath East Africa. Geology 28:599–602. doi: 10.1130/0091-7613(2000)28<599:SEFADU>2.0.CO;2

Pabich S, Vollmer C, Gussone N (2020) Investigation of crystal orientation patterns of foraminifer tests by Electron Backscatter Diffraction analysis. Eur J Mineral 32:613-622

Pilbeam LH, Nielsen TFD, Waight TE (2013) Digestion Fractional Crystallization (DFC): an Important Process in the Genesis of Kimberlites. Evidence from Olivine in the Majuagaa Kimberlite, Southern West Greenland. J Petrol 54:1399–1425. doi: 10.1093/petrology/egt016

Reid AM, Donaldson CH, Dawson JB, et al (1975) The Igwisi Hills extrusive “kimberlites”. Phys Chem Earth 9:199–218

Ritsema J, Nyblade AA, Owens TJ, et al (1998) Upper mantle seismic velocity structure beneath Tanzania, East Africa: Implications for the stability of cratonic lithosphere. J Geophys Res Solid Earth 103:21201–21213. doi: 10.1029/98jb01274

Rooney T, Girard G, Tappe S (2020) The impact on mantle olivine resulting from carbonated silicate melt interaction. Contrib to Mineral Petrol 175:1–15. doi: 10.1007/s00410-020-01694-0

Russell JK, Porritt LA, Lavallée Y, Dingwell DB (2012) Kimberlite ascent by assimilation-fuelled buoyancy. Nature 481:352–356. doi: 10.1038/nature10740

Seitz H-M, Woodland AB (2000) The distribution of lithium in peridotitic and pyroxenitic mantle lithologies — an indicator of magmatic and metasomatic processes. Chem Geol 166:47–64

Shaikh AM, Kumar SP, Patel SC, et al (2018) The P3 kimberlite and P4 lamproite, Wajrakarur kimberlite field, India: mineralogy, and major and minor element compositions of olivines as records of their phenocrystic vs xenocrystic origin. Mineral Petrol 112:609–624. doi: 10.1007/s00710-018-0562-2

Shaikh AM, Patel SC, Bussweiler Y, et al (2019) Olivine trace element compositions in diamondiferous lamproites from India: Proxies for magma origins and the nature of the lithospheric mantle beneath the Bastar and Dharwar cratons. Lithos 324–325:501–518. doi: 10.1016/j.lithos.2018.11.026

Shaikh AM, Tappe S, Bussweiler Y, et al (2020) Clinopyroxene and garnet mantle cargo in kimberlites as probes of Dharwar craton architecture and geotherms, with implications for post-1.1 Ga lithosphere thinning events beneath southern India. J Petrol 61(9):egaa087

Skinner EMW (1989) Contrasting Group I and Group II kimberlite petrology: towards a genetic model for kimberlites. In: Ross J et al. (eds.) Proceedings of the 4th international kimberlite conference, vol 1, Geological Society of Australia Special Publication 14, pp 528–544

Sobolev NV., Sobolev AV., Tomilenko AA, et al (2015) Paragenesis and complex zoning of olivine macrocrysts from unaltered kimberlite of the Udachnaya-East pipe, Yakutia: Relationship with the kimberlite formation conditions and evolution. Russ Geol Geophys 56:260–279. doi: 10.1016/j.rgg.2015.01.019

Sobolev NV, Logvinova AM, Zedgenizov DA, et al (2009) Lithos Petrogenetic significance of minor elements in olivines from diamonds and peridotite xenoliths from kimberlites of Yakutia. Lithos 112:701–713. doi: 10.1016/j.lithos.2009.06.038

Soltys A, Giuliani A, Phillips D (2018) Crystallisation sequence and magma evolution of the De Beers dyke (Kimberley, South Africa). Mineral Petrol 112, 503–518. doi: 10.1007/s00710-018-0588-5

Soltys A, Giuliani A, Phillips D, et al (2016) In-situ assimilation of mantle minerals by kimberlitic magmas - Direct evidence from a garnet wehrlite xenolith entrained in the Bultfontein kimberlite (Kimberley, South Africa). Lithos 256–257:182–196. doi: 10.1016/j.lithos.2016.04.011

Soltys A, Giuliani A, Phillips D, Kamenetsky VS (2020) Kimberlite Metasomatism of the Lithosphere and the Evolution of Olivine in Carbonate-rich Melts - Evidence from the Kimberley Kimberlites (South Africa). J Petrol 61. doi: 10.1093/petrology/egaa062

Stachel T, Harris JW, Brey GP (1998) Rare and unusual mineral inclusions in diamonds from Mwadui, Tanzania. Contrib to Mineral Petrol 132:34–47. doi: 10.1007/s004100050403

Stamm N, Schmidt MW (2017) Asthenospheric kimberlites: volatile contents and bulk compositions at 7 GPa. Earth Planet. Sci Lett 474:309–321

Sun J, Tappe S, Kostrovitsky SI, et al. (2018) Mantle sources of kimberlites through time: A U-Pb and Lu-Hf isotope study of zircon megacrysts from the Siberian diamond fields. Chem Geol 479:228–240

Tappe S, Budde G, Stracke A, et al (2020) The tungsten-182 record of kimberlites above the African superplume: Exploring links to the core-mantle boundary. Earth Planet Sci Lett 547:116473. doi: 10.1016/j.epsl.2020.116473

Tappe S, Foley SF, Jenner GA, et al (2006) Genesis of ultramafic lamprophyres and carbonatites at Aillik Bay, Labrador: A consequence of incipient lithospheric thinning beneath the North Atlantic Craton. J Petrol 47:1261–1315. doi: 10.1093/petrology/egl008

Tappe S, Massuyeau M, Smart KA, et al. (2021) Sheared peridotite and megacryst formation beneath the Kaapvaal craton: A snapshot of tectonomagmatic processes across the lithosphere–asthenosphere transition. J. Petrol 10.1093/petrology/egab046

Tappe S, Pearson DG, Nowell G, et al (2011) A fresh isotopic look at Greenland kimberlites : Cratonic mantle lithosphere imprint on deep source signal. Earth Planet Sci Lett 305:235–248. doi: 10.1016/j.epsl.2011.03.005

Tappe S, Romer RL, Stracke A, et al (2017) Sources and mobility of carbonate melts beneath cratons, with implications for deep carbon cycling, metasomatism and rift initiation. Earth Planet Sci Lett 466:152–167. doi: 10.1016/j.epsl.2017.03.011

Tappe S, Smart K, Torsvik T, et al (2018) Geodynamics of kimberlites on a cooling Earth: Clues to plate tectonic evolution and deep volatile cycles. Earth Planet Sci Lett 484:1–14. doi: 10.1016/j.epsl.2017.12.013

Tappe S, Steenfelt A, Heaman LM, Simonetti A (2009) The newly discovered Jurassic Tikiusaaq carbonatite-aillikite occurrence, West Greenland, and some remarks on carbonatite-kimberlite relationships. Lithos 112:385–399. doi: 10.1016/j.lithos.2009.03.002

Tappe S, Steenfelt A, Nielsen TFN (2012) Asthenospheric source of Neoproterozoic and Mesozoic kimberlites from the North Atlantic craton, West Greenland: new high-precision U-Pb and Sr-Nd isotope data on perovskite. Chem Geol 320–321:113–127

Tiberi C, Gautier S, Ebinger C, et al (2019) Lithospheric modification by extension and magmatism at the craton-orogenic boundary: North Tanzania Divergence, East Africa. Geophys J Int 216:1693–1710. doi: 10.1093/gji/ggy521

Tommasi A, Vauchez A, Ionov DA (2008) Deformation, static recrystallization, and reactive melt transport in shallow subcontinental mantle xenoliths (Tok Cenozoic volcanic field, SE Siberia). Earth Planet Sci Lett 272:65–77. doi: 10.1016/j.epsl.2008.04.020

Tovey M, Giuliani A, Phillips D, et al (2021) The spatial and temporal evolution of primitive melt compositions within the Lac de Gras kimberlite field, Canada: Source evolution vs lithospheric mantle assimilation. Lithos 392–393:106142. doi: 10.1016/j.lithos.2021.106142

Weeraratne DS, Forsyth DW, Fischer KM, Nyblade AA (2003) Evidence for an upper mantle plume beneath the Tanzanian craton from Rayleigh wave tomography. J Geophys Res Solid Earth 108:2427. doi: 10.1029/2002jb002273

Willcox A, Buisman I, Sparks RSJ, et al (2015) Petrology, geochemistry and low-temperature alteration of lavas and pyroclastic rocks of the kimberlitic Igwisi Hills volcanoes, Tanzania. Chem Geol 405:82–101. doi: 10.1016/j.chemgeo.2015.04.012

Figure Captions

Fig. 1. Location (left side) and geological map (right side) of the ca. 12 ka Igwisi Hills kimberlite volcanoes. The inset photograph shows a polished kimberlite 'lava' rock sample for which the location is given on the map with star symbol. Note the abundant subrounded to rounded dunitic nodules and olivine macrocrysts.

Fig. 2. Plane-polarized light (PPL) images of Igwisi Hills kimberlite samples (a-b) and cross-polarized light images of dunitic nodules (c-f). Coloured arrows in (a) and (b) mark the veins of melt inclusions (now quenched as carbonates) trapped in the matrix. Note the olivine crystals and calcite laths in the kimberlite matrix defining a flow texture. (c-f) Dunitic nodules with anhedral host olivine grains that are cross-cut by subhedral to anhedral olivine neoblasts. Note that virtually all dunitic nodules are subrounded. In Panel (e), olivine neoblasts are aligned along an inter-grain fracture but otherwise occur inside or along the margins of host olivine grains (c, d, f). Neoblasts – N.

Fig. 3. (a) Dunitic nodule showing cracks of different generations (i.e., sealed, healed and curvilinear) and melt inclusions plus minute olivine neoblasts along the host olivine grain margins. (b) Recrystallized dunitic nodule showing cracks (red arrow) running from the olivine neoblasts into the host olivine grain. (c) BSE image of an olivine phenocryst showing spinel inclusions that are aligned along the olivine crystal growth planes. Neoblasts – N.

Fig. 4. (a) Forsterite versus NiO (wt.%) and (b) forsterite versus CaO (wt.%) contents of various olivine populations (host olivine in dunitic nodule, macrocryst core, neoblast, phenocryst, inner zone and rim) identified in the Igwisi Hills kimberlite lavas. The fields for olivine from granular (pink) and sheared (black dotted line) peridotites are after Giuliani (2018).

Fig. 5. Concentrations of minor and trace elements in olivine (in ppm): Ca (a), Mn (b), Al (c), Sc (d), Zn (e) and Gd (f) plotted against Ni for different olivine populations in the Igwisi Hills kimberlite lavas. Data for olivine megacrysts from the Monastery kimberlite on the Kaapvaal craton are from Howarth (2018).

Fig. 6. EBSD texture component image (with the blue colour of the host olivine as reference orientation), crystallographic pole figures, and element maps (Mg, Fe, Ni, Ca) shown together with a BSE image of the IH57BG1 dunitic nodule from the Igwisi Hills kimberlite lavas. In the BSE image, olivine cores are circled by red dotted lines, neoblasts by yellow dotted lines, and inner zones of olivine by black dotted lines. Note that the crystallographic orientation of the olivine neoblasts is mostly random and differs from the orientation of the host olivine grains (shades of blue). The inner zones of olivine crystals are associated with olivine neoblasts. Numerous carbonate-rich melt inclusions occur along grain boundaries and fractures.

Fig. 7. EBSD texture component image, crystallographic pole figures, and element maps (Mg, Fe, Ni, Ca) together with a BSE image of the IH57BG2 dunitic nodule from the Igwisi Hills kimberlite lavas (olivine core – red dotted line; neoblasts – yellow dotted lines; inner zones of olivine – black dotted lines). Note that the crystallographic orientation of the olivine neoblasts is mostly random and differs from the orientation of the host olivine grains (shades of blue). The host olivine grains show kink banding (see the lower EBSD map) and contain Cr-rich phlogopite (phl) inclusions (marked in the BSE image). Note that the olivine rim on the left edge also shows a

deformation texture. Carbonate-rich melt inclusions are exclusively associated with the inner zones of olivine crystals. Note further that the rims cut through olivine neoblasts establishing a relative sequence of petrogenetic events.

Fig. 8. BSE images of representative dunitic nodules (a, b, d) and olivine macrocrysts (c) from the Igwisi Hills kimberlite lavas. Note the strongly resorbed olivine cores and also the melt inclusions that occur along fractures in olivine. Note further that the majority of the melt inclusions occur inside the inner zones of olivine, which are relatively Fe-rich compared to the resorbed olivine cores. *cal – calcite, spl – spinel, grt – garnet.*

Fig. 9. Mn versus Al (a), Zr versus Sc (b), and Al versus V (c) diagrams for olivine from the dunitic nodules (host grains and neoblasts) and macrocrysts in the Igwisi Hills kimberlite lavas. The layouts of panels (a) and (b) are after De Hoog et al. (2010), whereas panel (c) is adopted from Bussweiler et al. (2017). Note that all host olivine grains of the dunitic nodules and the majority of the olivine macrocryst cores show an affinity to garnet-bearing peridotite sources.

Fig. 10. Aluminum-in-olivine temperature versus pressure for host olivine grains of the dunitic nodules and olivine macrocryst cores from the Igwisi Hills kimberlite lavas. The temperatures are calculated using the formulation by Bussweiler et al. (2017) and have been projected onto the 41 mW/m^2 modern geotherm of the Tanzania craton as determined by Gibson et al. (2013). Oxidized and reduced dehydration solidus curves are after Green and Falloon (1998). The graphite–diamond phase transition curve is after Day (2012). The fields for the various primitive mantle-derived melt types (i.e., basanite, nephelinite, melilitite, leucitite) are taken from Green and Falloon (1998).

Fig. 11. (a, b) Typical olivine macrocrysts from the Benfontein calcite kimberlite sill complex on the Kaapvaal craton, redrawn from Howarth and Taylor (2016, their Figures 5a and 6d). Note the continuous (a) and discontinuous

(b) transition zones (so-called ‘inner zones’ in our work). In panel (b), the olivine core shows a sharp contact against the melt zone because the transition/equilibration zone is partly missing.

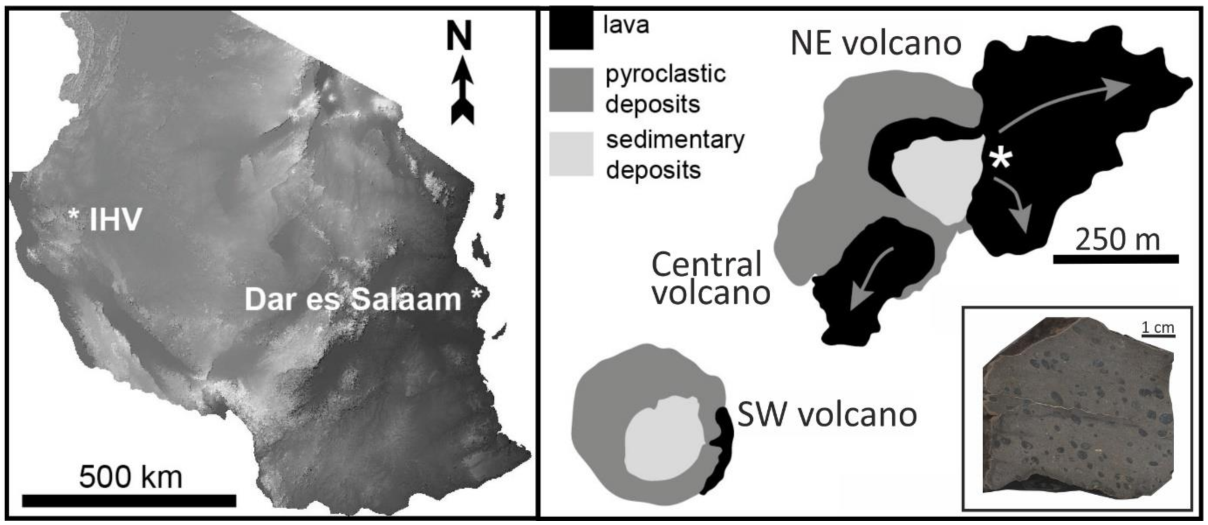

Fig. 1. Location (on left side) and geological map (on right side) of the Igwisi Hills volcanic system. Inset photograph shows the polished sample of the kimberlite lava for which location is given on the left-side map (star symbol). Note the subrounded to rounded shaped abundant olivine grains/nodules in the sample.

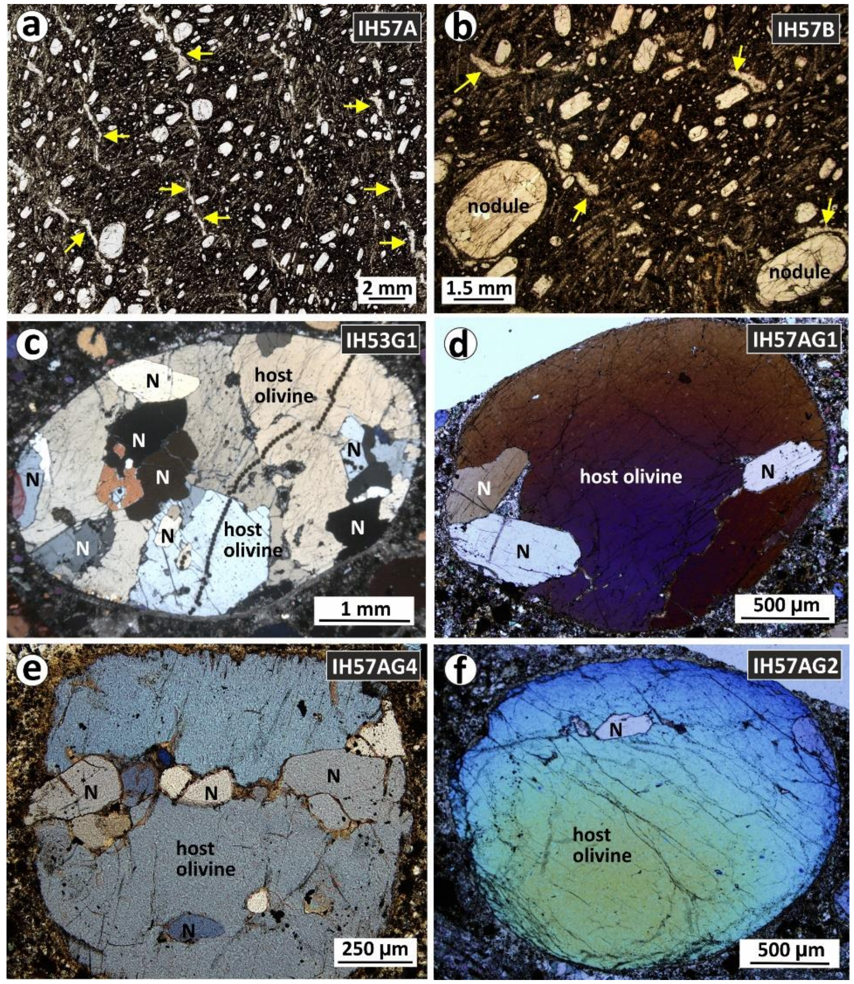

Fig. 2. Plane polarized light (PPL) images of Igwisi Hills kimberlite samples (a-b) and crossed Nicol images of dunitic nodules (c-f). Yellow coloured arrows in (a) and (b) images mark the veins of melt inclusions (now quenched as carbonates) trapped in the matrix. Also, note that the olivine crystals and calcite laths in the matrix show a distinct flow texture. (c-f) Dunitic nodules with anhedral host olivines cross-cut by subhedral to anhedral neoblasts (N). Note that virtually all nodules are subrounded. In figure (e) neoblasts are aligned along an inter-granular fracture and otherwise occur inside or along the margin (c, d, f).

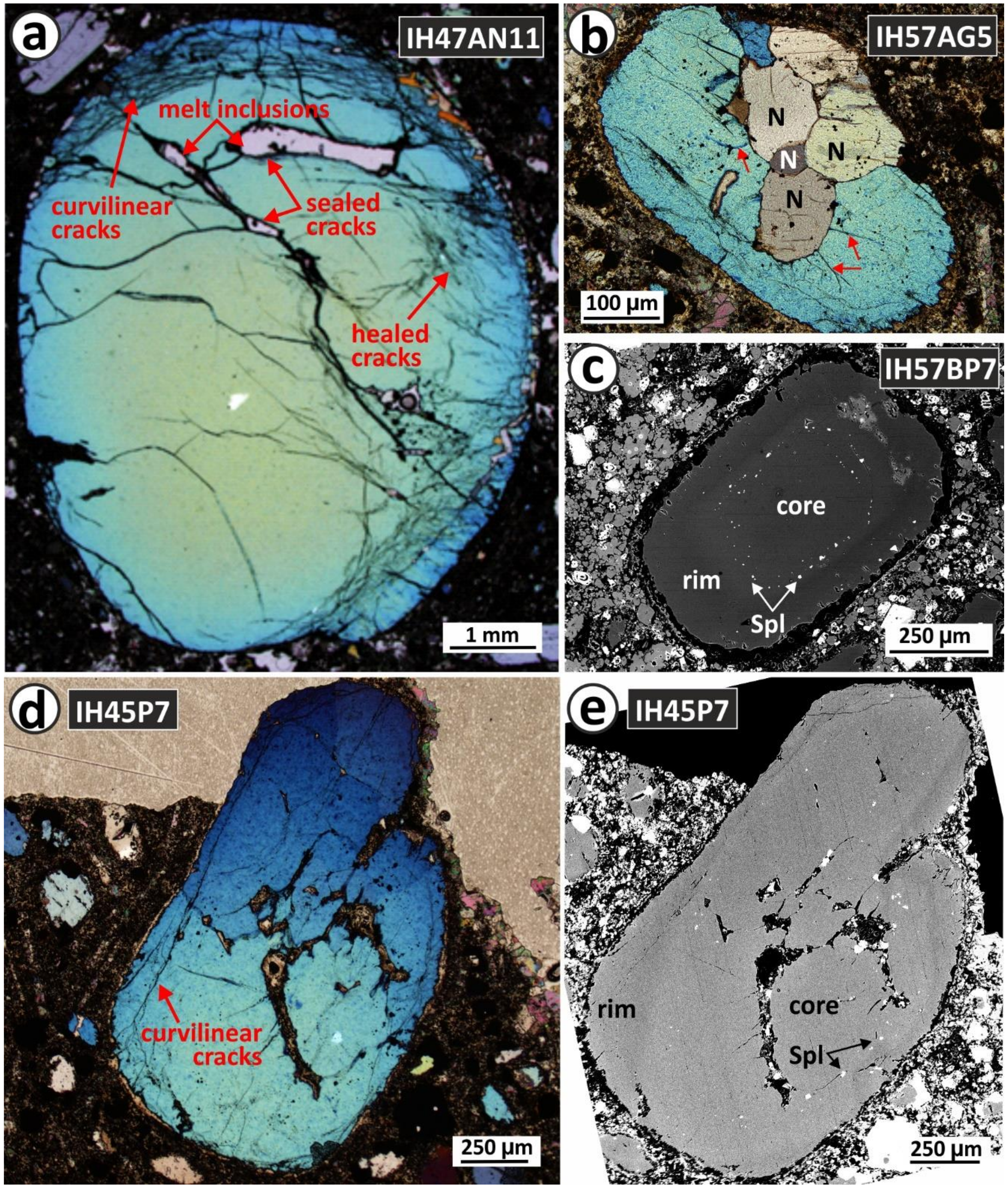

Fig. 3. (a) Olivine nodule showing cracks of different generations (sealed, healed and curvilinear) and melt inclusions along with tiny neoblasts (N) along the margin. (b) Recrystallized olivine nodule showing cracks (red arrow) running away from the neoblasts into the host. (c) BSE image of olivine phenocryst showing inclusions of spinel crystals aligned along the growth planes. Crossed polar image (d) and BSE image (e) of olivine phenocryst showing the hopper growth structure.

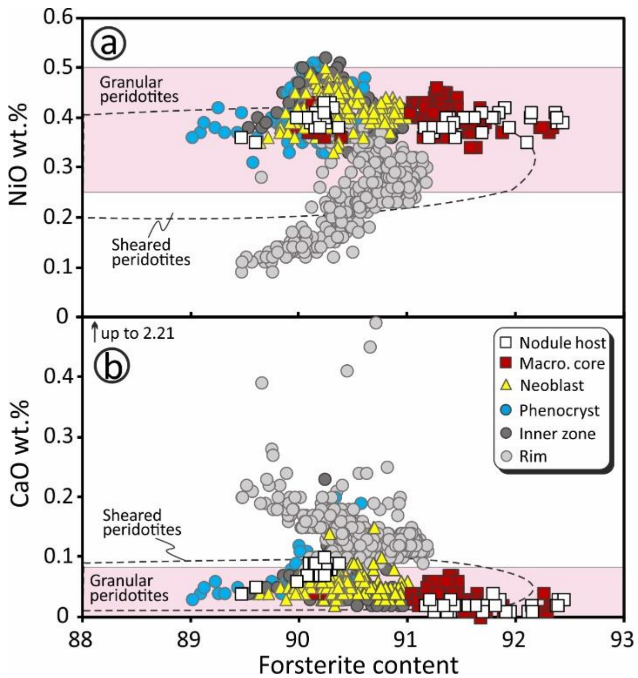

Fig. 4. (a) Forsterite versus NiO (wt.%) and (b) Forsterite versus CaO (wt.%) contents of various populations of olivine (host olivine in nodule, macrocryst core, neoblast, phenocryst, inner zone and rim) identified in Igwisi Hills kimberlite samples. The field for granular (pink colored) and sheared (black dotted line) peridotites is after Giuliani (2018).

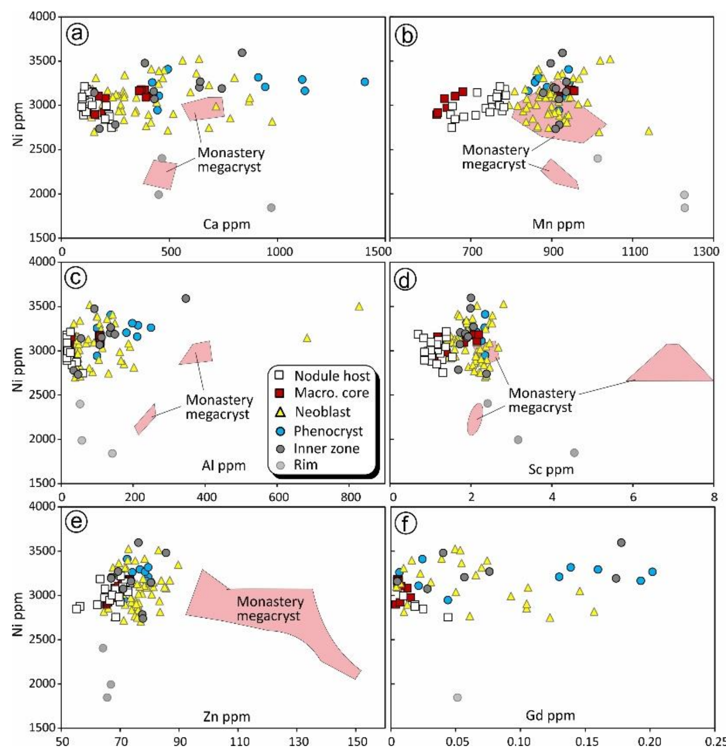

Fig. 5. Concentrations of trace elements (in ppm) Ca (a), Mn (b), Al (c), Sc (d), Zn (e) and Gd (f) plotted against Ni for different populations of olivine from the Igwisi Hills kimberlite. Trace element data for the Monastery megacryst are from Howarth (2018).

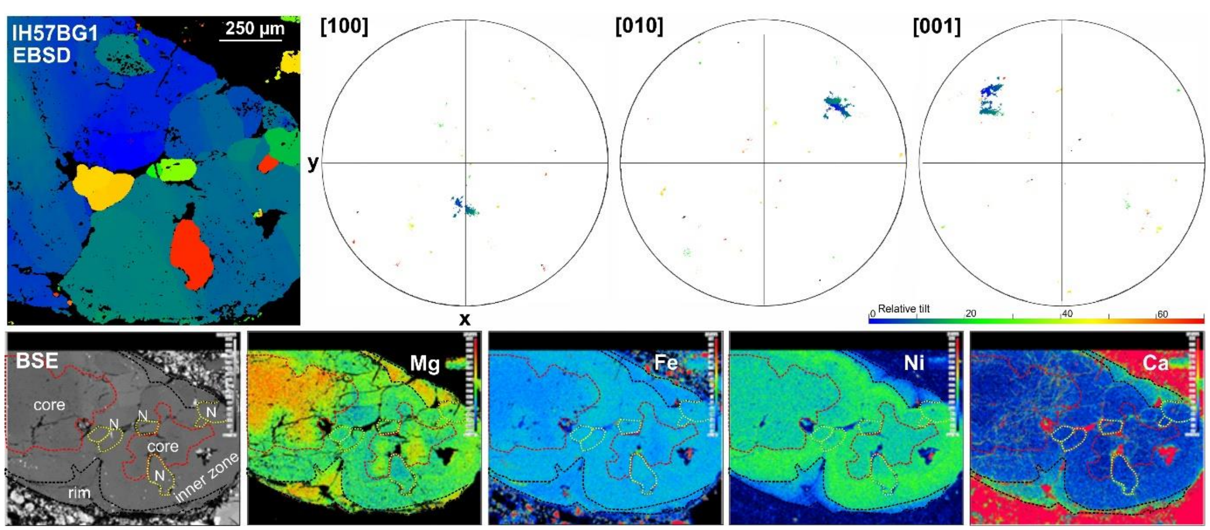

Fig. 6. EBSD texture component image (with the blue colour of the host olivine as reference orientation), crystallographic pole figures, and elemental (Mg, Fe, Ni and Ca) maps along with Back Scattered Electron (BSE) image of IH57BG1 dunitic nodule from the Igwisi Hills. In BSE image, neoblasts are marked with yellow dotted

lines, core with red dotted line and inner zones with black dotted lines. Note that crystallographic orientation of neoblasts (other than bluish colour) is random and different than that of the host anhedral olivine (bluish colour). Also, inner zones are associated neoblasts and numerous melt inclusions (mostly carbonates) are formed along intergranular boundaries and fractures.

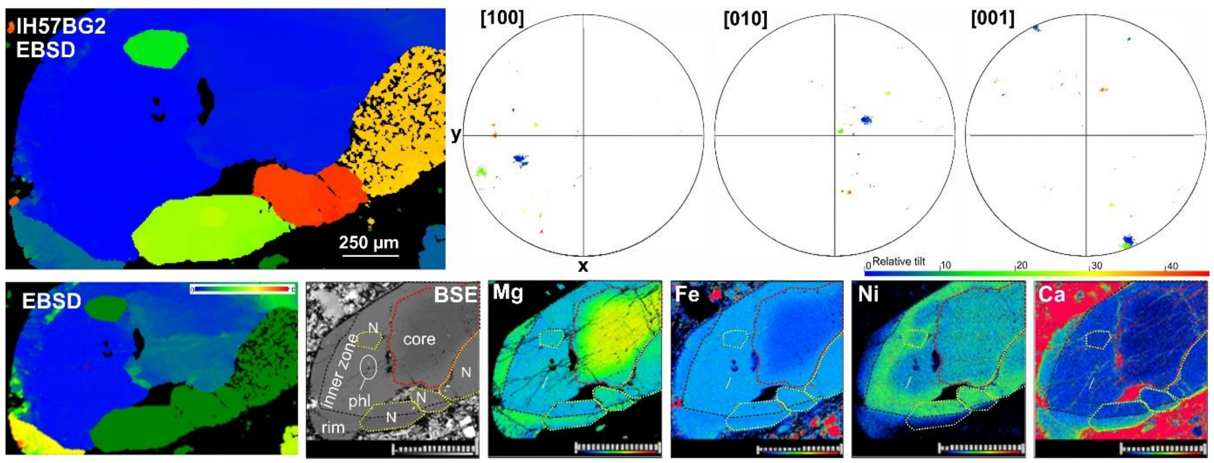

Fig. 7. EBSD texture component image, crystallographic pole figures, and elemental (Mg, Fe, Ni and Ca) maps along with BSE image (with neoblasts marked with yellow dotted lines, core with red dotted line and inner zones with black dotted lines) of IH57BG2 dunitic nodule from the Igwisi Hills. Note that crystallographic orientation of neoblasts (other than bluish colour) is random and different than that of the host anhedral olivine (bluish colour). Anhedral olivine also shows kink banding (shown in the lower small EBSD map) and contains Cr-rich phlogopite (phl) inclusion (marked in BSE image), while the rim on the left edge also shows deformation textures. Melt inclusions (mostly carbonates) are exclusively associated with the inner zone. Also, note that rim cuts indiscriminately to the neoblast indicating their post-neoblast formation.

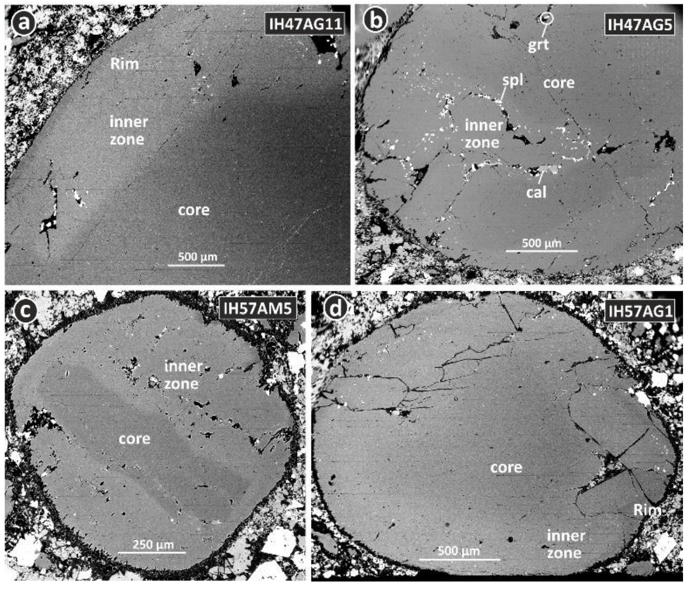

Fig. 8. BSE images of dunitic nodules (a, b, d) and olivine macrocryst (c) showing extensively resorbed cores and melt inclusions formed along the pre-existing fractures. Note that the majority of the inclusions occur inside the inner zone that are relatively Fe-rich in composition compared to the extensively resorbed cores. Abbreviations: cal = calcite, spl = spinel and grt = garnet.

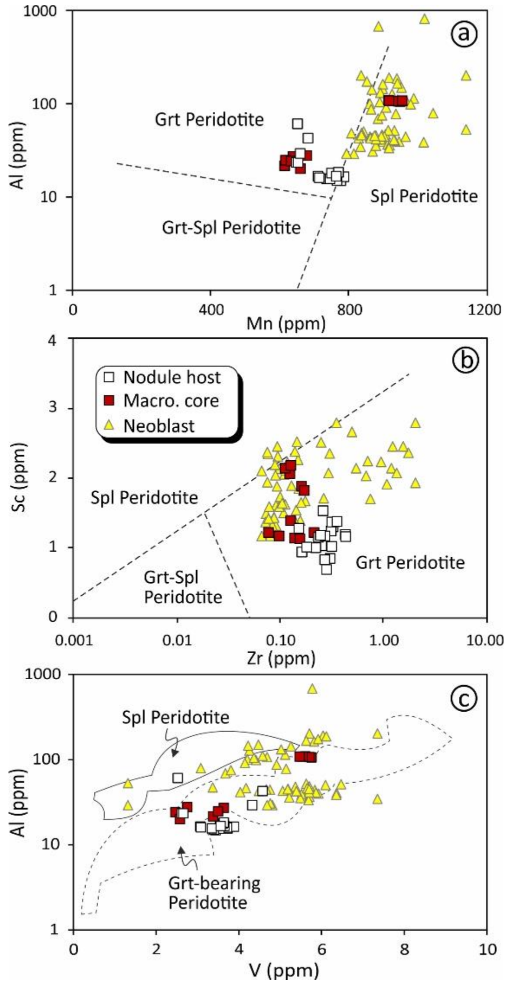

Fig. 9. Mn versus Al (a), Zr versus Sc (b) and Al versus V (c) discrimination plots for dunitic nodules (both host olivine and neoblasts) and olivine macrocrysts. Plots (a) and (b) are after De Hoog et al. (2010) and plot (c) is after Bussweiler et al. (2017). Note that all host olivines in nodules and the majority of macrocryst cores show a clear affinity towards a garnet-bearing source rock and neoblasts show enrichment in these trace elements.

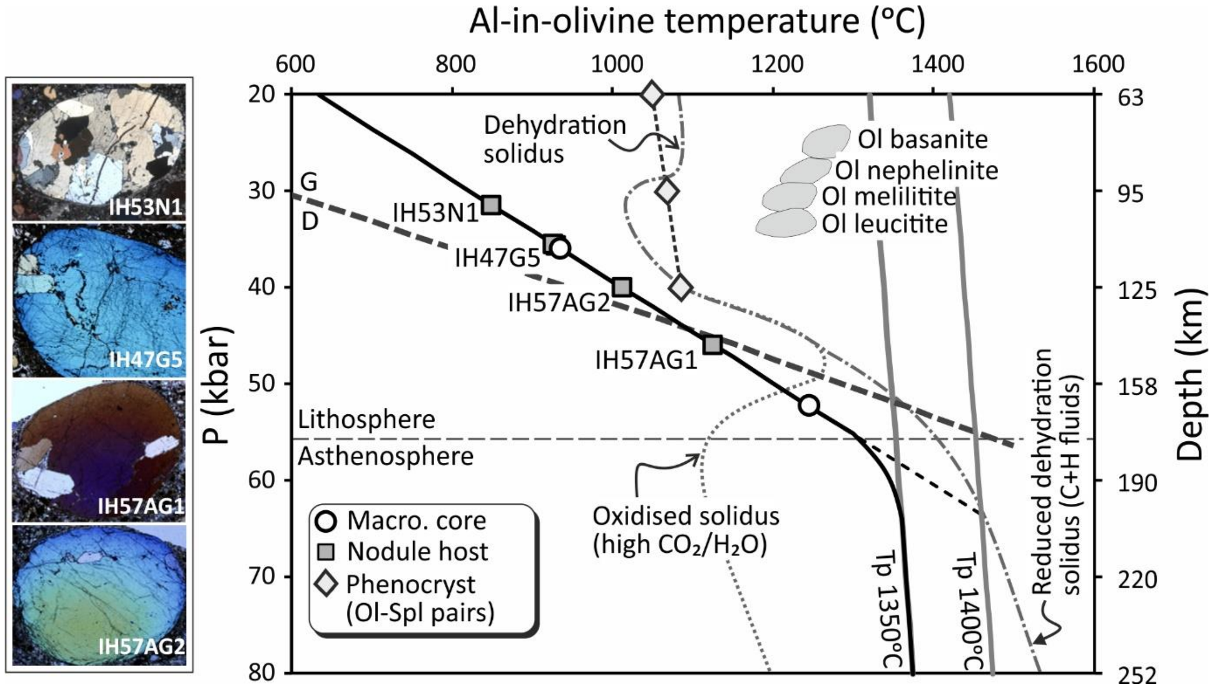

Fig. 10. Al-in-olivine temperatures (after Bussweiler et al., 2017) versus pressure plot for host olivine in nodules (inset figures in the left side) and core of olivine macrocrysts from Igwisi Hills kimberlite. Al-in-olivine temperatures are projected onto the geotherm of 41 mW/m2 (after Gibson et al., 2013). Oxidized and reduced dehydration solidus are after Green and Falloon (1998). Graphite and diamond transition after Day (2012) and fields of various olivine-bearing magmas (basanite, nephelinite, melilitite and leucitite) are after Green and Falloon (1998).

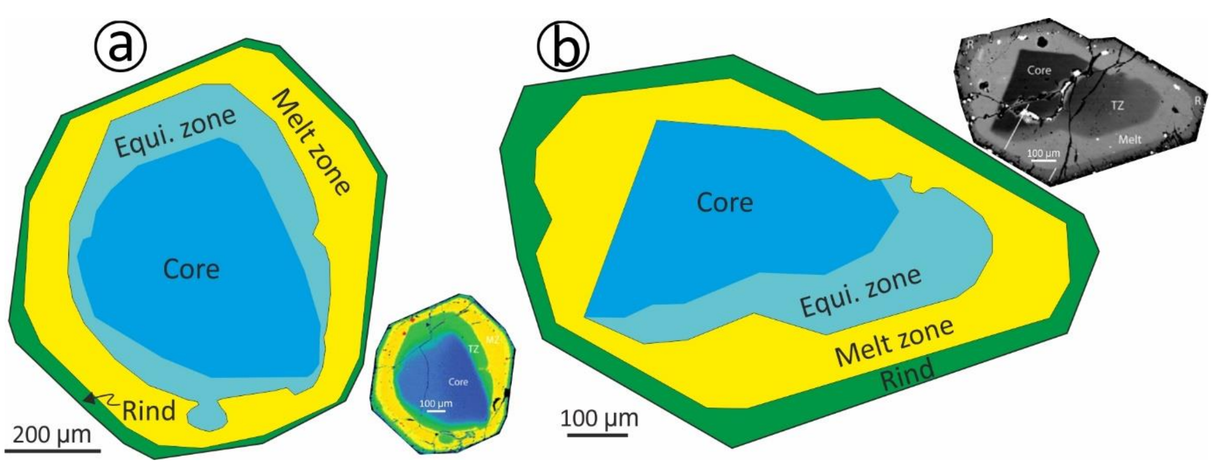

Fig. 11. (a, b) Olivine macrocrysts from Benfontein kimberlite redrawn from Howarth and Taylor (2016, Fig.5a and 6d). Note the continuous transition zone (inner zones in this work) with resorption features in figure (a) and

discontinuous in figure (b). In figure (b), core shows sharp contact with melt zone at western-end where transition zone is missing.